

June 20, 2020

Dear Editor,

Thanks for your efforts on this manuscript. We have received comments from the reviewers of our manuscript, and we would like to thank the reviewers for their careful reading and their insightful comments. To address the reviewers' comments, we have revised the manuscript, and the revised text is highlighted in red.

Best Regards,

Xuexi Tie

Reply to Anonymous Referee #1

Thanks for the reviewer's helpful comments. We have given our point-to-point response to your comments and suggestions in the revised manuscript. To carefully address the comments of the reviewer, we add more content and figures. We would like to think that the revised manuscript is greatly improved after addressing the reviewer's comments.

General comments:

In this manuscript, the authors focus on the effect of warming Tibetan Plateau on air quality in the Sichuan Basin, China. Specifically, they address the 2°C warming causes an increase in the PBL height and a decrease in the relative humidity in the basin. The elevated PBL height strengthens vertical diffusion of PM2.5, while the decreased RH significantly reduces secondary aerosol formation. The authors highlight that the recent warming plateau has improved air quality in the basin. The results of this work are based on the WRF-Chem simulations and extensive observation. The analysis is mostly sound, the manuscript is well written, but some details need clarify. I recommend a minor revision with my comments listed below.

Specific comments:

Comment 1. In line151, please further explain what does “‘top-down’ method” means here and how to use the ‘top-down’ method to constrain the emission inventory via comparing the simulations with the measurements?

Response: The ‘top-down’ method is to compare the simulated value with the observed value time and again until the simulated values, including the averaged level and the trend, are close to the observed ones. Generally, we use mean bias (MB), root mean square error (RMSE), and index of agreement (IOA) to evaluate the model performance. The higher the IOA, the closer the simulated value is to the observed value. In this study, the statistical indices of agreement (IOAs) of pollutants (O₃, CO and PM_{2.5}) are greater than 0.7.

The ‘bottom-up’ emission inventory used in this study is constructed by national and provincial emission factors and activity data based on a statistical approach, so it is difficult to obtain accurate activity data. Also, the emission factors representative at a local level is difficult to

measured. Therefore, the spatial pattern of the inventory at a local level needs to be improved. In addition, the ‘bottom-up’ emission inventory is not updated every year. In practice, the ‘bottom-up’ emission inventory is used to drive the model, and the ‘top-down’ method is used to constrain the emission. Top-down constraints on emissions is helpful to improve the accuracy of the ‘bottom-up’ emission inventory. The detailed introduction of these two approaches are referred to Zhang et al. (2009) and Fu et al. (2012).

In the revised version, we have added a brief introduction to the ‘top-down’ method, and the text is “*The emission inventory is constructed by a ‘bottom-up’ approach based on national and provincial activity data and emission factors. To improve the emission inventory accuracy, we use a ‘top-down’ method here to constrain the emission inventory. We compare the simulated value with the measured value time and again until the simulations are close to the measurements.*” In lines 151 - 155.

Fu, T. M., Cao, J. J., Zhang, X. Y., Lee, S. C., Zhang, Q., Han, Y. M., et al. (2012). Carbonaceous aerosols in China: top-down constraints on primary sources and estimation of secondary contribution. *Atmospheric Chemistry and Physics*, 12(5), 2725–2746. <http://doi.org/10.5194/acp-12-2725-2012>

Zhang, Q., Streets, D. G., Carmichael, G. R., He, K. B., Huo, H., Kannari, A., et al. (2009). Asian emissions in 2006 for the NASA INTEX-B mission. *Atmospheric Chemistry and Physics*, 9(14), 5131–5153. <http://doi.org/10.5194/acp-9-5131-2009>

Comment 2. In line 164-165, in the configuration of the sensitivity simulation, how to set the temperature increment to 2K? Is it just increase the temperature in all levels and all grids of the model above Tibetan Plateau (TP)? Does the 2K increment set at the beginning of model simulation or need nudging in every step of the simulation? Are the temperature increment same in verticals or just at the surface?

Response: We have given a detailed description for the 2K sensitivity simulation in the revised version. According to the ERA-interim reanalysis data, the warming is only happening in the troposphere (600 hPa - 250 hPa). As a result, in the sensitivity simulation, we set the 2K increment in the troposphere (600 hPa - 250 hPa) over the Tibetan Plateau. In order to ensure a persistent influence of the 2K increment, we add the 2K increment at the initial and boundary conditions of the model, and also drive the initial condition with a 2K increment every day.

These texts are added in the revised manuscript. “According to the meteorological records at weather stations, surface air temperature risen by an average of 2°C from 2013 to 2017 over the Tibetan Plateau (Table S1). ERA-interim reanalysis data also show that the troposphere (600hPa - 250hPa) over the plateau is warming during the 2013-2017 period, and the temperature increment shows a parabolic pattern with the altitude, by an average increase of ~2°C (Figure S1). Thus, we design a sensitivity simulation, with a temperature increase of 2°C in the troposphere over the plateau. In the model, we set to the 2°C warming in the initial and boundary fields. In order to ensure a persistent influence of the 2°C warming, we drive the initial field with a 2°C increment every day. Then, by comparing the difference between the sensitivity simulation and the baseline simulation, we determine the impact of the 2°C warming over the Tibetan Plateau on air quality in the Sichuan Basin.” In Lines 167 - 178.

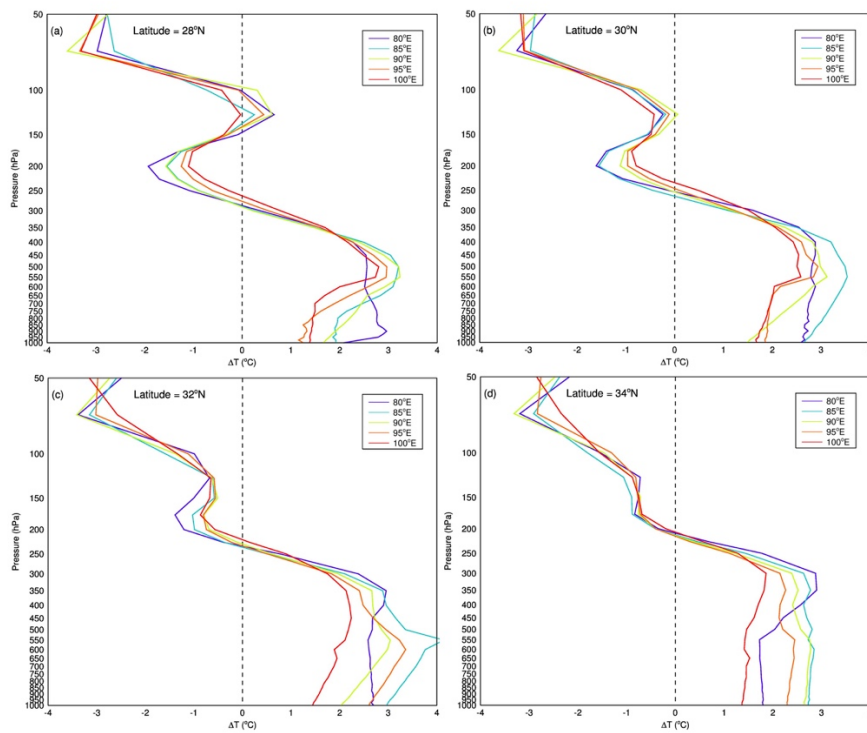


Figure S1 Vertical profile of temperature change along the longitude (80°E - 100°E) covering the plateau at 28°N, 30°N, 32°N and 34°N, ΔT is calculated by the annual temperature increase rate from 2013 to 2017 multiplying by the number of years ($N = 5$). Noted that the temperature in the troposphere over the Tibetan Plateau (600 hPa - 250 hPa) is inhomogeneously warming by 0 - 4 °C from 2013 to 2017, and we take an average warming increase of 2 °C.

Comment 3. In line 231-232, is it correct here “the overestimated PM2.5 concentration is mainly caused by the overestimated wind speed”? Or underestimated wind speed?

Response: Yes. We have explained that the overestimated PM_{2.5} concentration here is mainly related to the wind departure in detail, including of an overestimated wind speed and a departure of wind direction. Figure S4 shows that the simulated temperature and humidity are well consistent with the observed, but the simulated winds are not consistent with the observed. Observational wind speed concentrates in the range of 1 - 2 m s⁻¹ (the average wind speed is 1.3 m s⁻¹), obviously lower than the simulated wind speed (mostly higher than 2 m s⁻¹, the average wind speed is 2.0 m s⁻¹,). The observed prevailing wind is northerly wind while the simulated is mainly easterly wind. Figure S6a shows that PM_{2.5} concentration is lower in the north to Sichuan Basin while higher in the east to the basin. Therefore, the simulated high PM_{2.5} concentration is mainly caused by a wind departure, which results in a false transport from the east to the basin. To clarify the explanation, we have revised the text as follows “*During the period of Jan 17th to Jan 20th, the observed wind speed concentrates in the range of 1 - 2 m s⁻¹, with an average of 1.3 m s⁻¹, while the simulated wind speed is obviously higher, with an average of 2.0 m s⁻¹ (Figure S3). The observed prevailing wind is northerly wind while the simulated prevails easterly wind. Figure S6a shows that PM_{2.5} concentration is lower in the north to the Sichuan Basin while higher to in the east to the basin. Therefore, the overestimated PM_{2.5} concentration is mainly caused by the departure of winds, which results in a false transport from the east to the basin.*” In lines 241 - 249.

Comment 4. Could you further explain the thermodynamic reasons of the winds and PBLH changes due to 2K warming over TP in figure 7 and the description in line 263- 269 “easterly winds over the basin enhance while westerly wind over the plateau weaken. . . . northerly winds over the basin slightly enhance,”?

Response: Yes, we have added the analysis of pressure gradient to explain the changes in winds (Figure 8, a new figure). The further explanation is as follows: “*Wind patterns show that easterly winds over the basin enhance while westerly wind over the plateau weaken (Figure S6 and Figure 7). We further compare the difference in the surface pressure between the baseline and sensitivity simulations, and find out that surface pressure over the plateau and the basin all decreases when the plateau warms by 2°C (Figure 8a and 8b). Over the plateau, the pressure drop has a decrease characteristic from west to east (Figure 8c), which results in a decreased pressure gradient and a weakened westerly wind. While in the basin, the pressure drop is less than the plateau. This leads to an increased pressure gradient from the basin to the plateau, inducing an intensified easterly wind. The enhanced easterly wind causes an increased transport of PM_{2.5} from the basin to the plateau. On the other hand, the weakened*

westerly wind and the enhanced easterly wind are convergent at the border between the plateau and the basin (Figure 7), jointly leading to an increase in $PM_{2.5}$ concentration at the eastern edge of the plateau. Additionally, northerly winds over the basin slightly enhance, conducive to diluting the air and reducing $PM_{2.5}$ concentration. Both easterly winds transport and northerly winds dilution are favorable for a reduction of $PM_{2.5}$ concentration in the basin.” In lines 278 - 291.

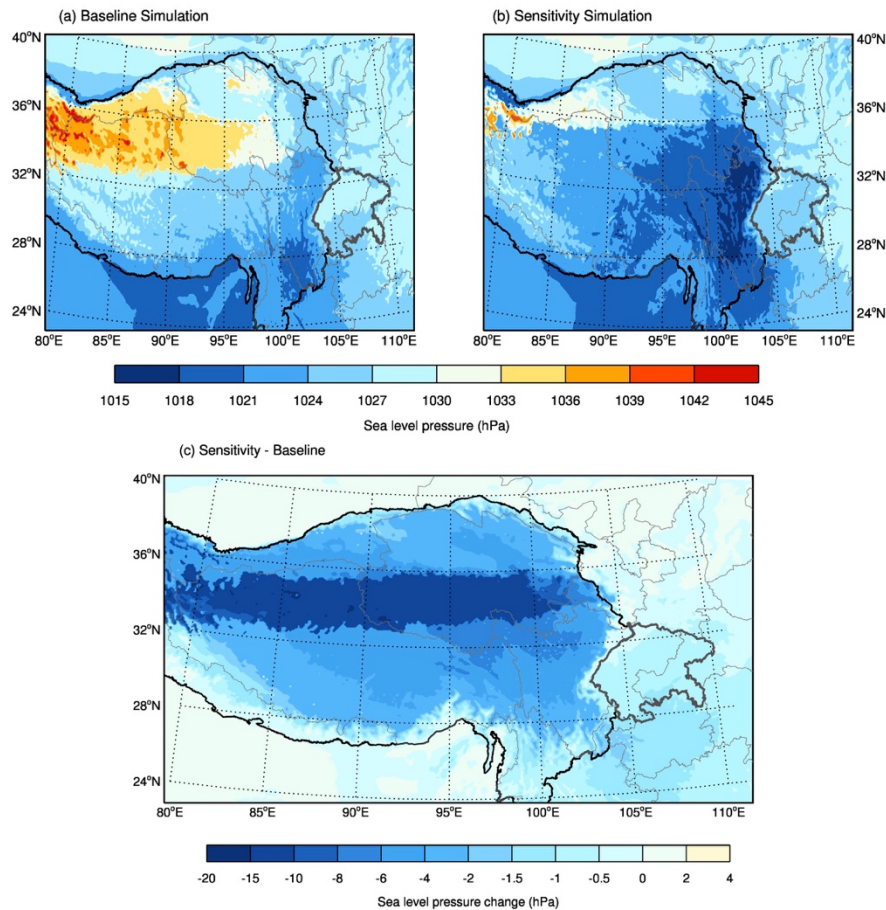


Figure 8 Comparison of spatial distributions of sea level pressure (SLP) between the (a) baseline simulation and (b) sensitivity simulation over the Tibetan Plateau and Sichuan Basin. (c) The SLPs over the plateau and basin decrease while the plateau becomes 2°C warming.

Comment 5. In line 293-295, similarly, could you further explain the mechanism of “a maximal temperature reduction located at 1.5 km to 3 km above the ground (Figure 9a)”?

Response: We have added the explanation: “*This is probably due to a sharp topography decrease (from ~ 5 km in the plateau to < 1 km in the basin) that leads to a warm plume via subsidence. In the basin, there is a decrease in the temperature from the surface to ~ 4 km, with a maximal temperature reduction (1 - 2°C) located at 1.5 km to 3 km above the ground (Figure 10a). We speculate that changes in the surface pressure can account for the maximal*

temperature reduction here. After the 2°C warming, surface pressure decreases in the basin (Figure 8), which produces more convergent airflow (as shown in Figure 7). The strengthened convergent airflow induces an intensified ascending motion, conducive to a reduction of temperature in the basin. As a result, the zone where the maximal temperature drop appears, overlaps with the zone with the maximal ascending motion. Furthermore, the intensified updraft increases the vertical temperature gradient and the instability in the lower troposphere of the basin, thereby causing a higher PBL height than that in the non-warming case (Figure 10b). On the contrary, the change in vertical temperature profile leads to a decreased vertical temperature gradient and increased thermal stability in the lower troposphere of the plateau, in which the PBL height decreases.

On the other hand, the convergent airflows by a weakened westerly wind over the plateau and a strengthened easterly wind in the basin (shown in Figure 8) triggers an ascending motion on the east side of the plateau, which is also beneficial to the development of the PBL height in the basin. Consequently, the elevated PBL facilitates vertical diffusion, leading to a reduction in PM_{2.5} concentration over the basin.” In Lines 313 - 332.

Comment 6. Related to comments 4 and 5, the paragraph from line 302-311 did not make very clear discussion on the changes of wind and temperature gradient. I suggest the comparison of the changes of pressure-difference between TP and basin, and see the circulation changes could easily explain the issues in comments 4 and 5.

Response: Thanks for your suggestions, in the revised manuscript, we have re-written the paragraph, and the text is referring to the response to Comment 5.

Comment 7. I don’t think the ascending motion in this study is similar to the plateau “heat pump” effect raised by Lau (2016)

Response: Yes, they are not the same. Here, we consider of the reviewer’s comment, and have deleted this statement that the ascending motion in this study is similar to that in the EHP mechanism.

Elevated Heat Pump (EHP) hypothesis proposed by Lau and Kim (2006) illustrate that absorbing aerosols (dust and black carbon) heat up the air over the south slope of the Tibetan Plateau, inducing an ascending motion in lower troposphere and a positive temperature

anomaly in the mid-to-upper troposphere over the TP. According to the mass continuity principle, the air divergent in upper level and the air convergent in lower level, which further strengthens the upward motions. Under the circumstance, low-level convergence draws more warm and moist air from South Asia to increase monsoon rainfall. This thermodynamic mechanism shows that the heated plateau acts as an elevated heat pump.

In the present study, the temperature over the Tibetan Plateau rises by 2°C, which triggers an upward airflow on the eastern edge of the plateau. We would like to think that the role of the 2°C warming over the TP is similar to the positive temperature anomaly induced by absorbing aerosols in the EHP mechanism. Consequently, the 2°C warming leads to a convergent airflow and an ascending motion on the east edge of the plateau. The difference is that the EHP mechanism happens in the north-south direction, and our study explains the similar thermodynamic processes in the east-west direction.

Technical corrections:

Comment 8. I am misleading by the figure 6 in the first look and regards they are pie charts in percentage of species. Plot them as columns could be better.

Response: We have modified Figure 6 by a column chart, seen Figure 6 in the revised version.

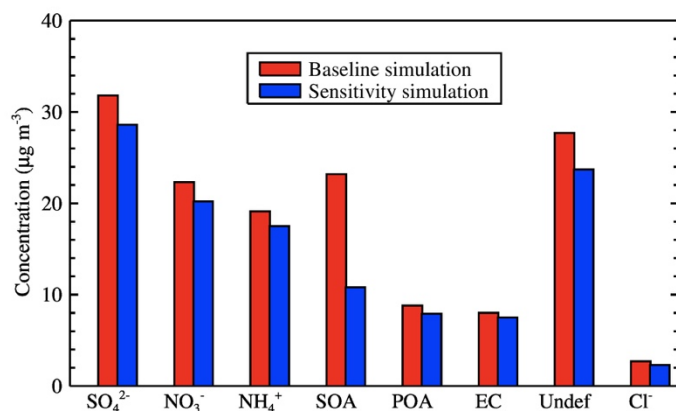


Figure 6 Comparison of chemical composition of PM_{2.5} concentration between the baseline simulation (red bar) and sensitivity simulation (blue bar) over the Sichuan Basin.

Comment 9. Setting figure 11 as figure 10c is reasonable.

Response: We have combined Figure 10 and Figure 11 together, and labeled Figure 11 in the revised version.

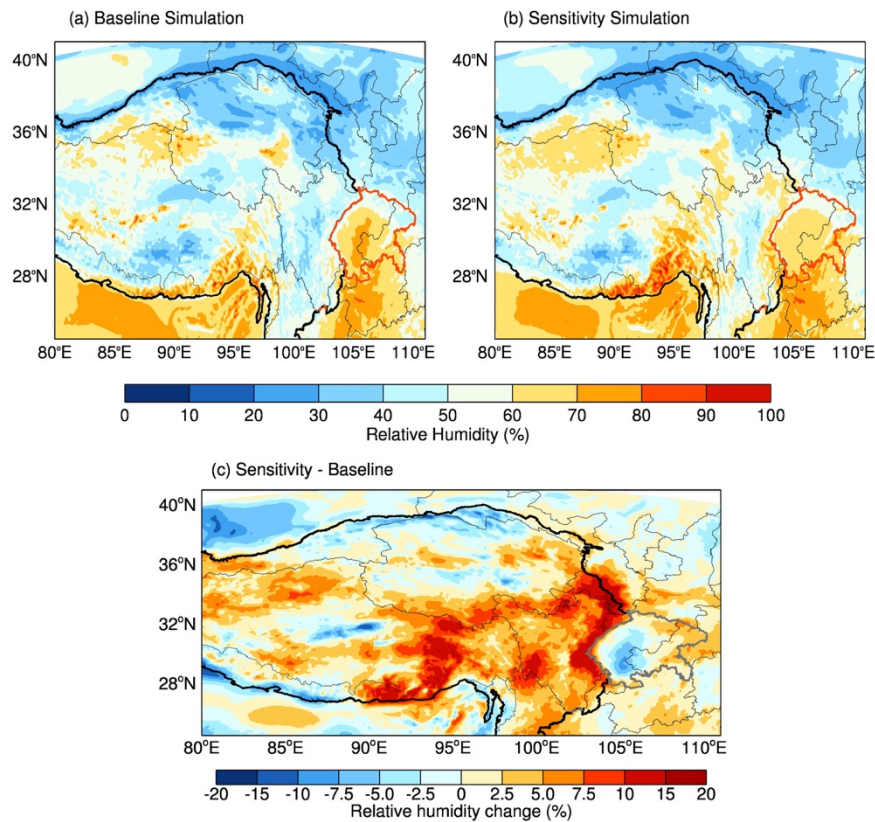


Figure 11 Comparison of spatial distributions of relative humidity (RH) between the (a) baseline simulation and (b) sensitivity simulation over the Tibetan Plateau and Sichuan Basin. (c) Spatial changes in RH after the plateau becomes 2°C warming, and the positive shows the RH increases while the negative shows the RH decreases.

Reply to Anonymous Referee #3

Thanks for the reviewer's helpful comments. We have given our point-to-point response to your comments in the revised manuscript.

General comments:

This paper investigated the role of warming Tibetan Plateau on winter air quality in the Sichuan Basin, China. This paper has indicated that the air temperature in winter over the TP has risen by 2 degrees from 2014 to 2017. Then the authors used sensitivity experiments to examine the influence of the warming TP on air quality in the Sichuan Basin. This paper is well written and well organized. However, this manuscript has not provided any physical explanations for the linkage between warming TP and less air quality in Sichuan Basin. In fact, I doubt that the relation between warming TP and less air pollution is not a cause-and-effect relation other than a companion relation caused by atmospheric circulation. Based on the following comments, I will not recommend publication for this manuscript at current situation. Of course, the resubmission is encouraged.

Major comments:

Comment 1. The description on the experiment design is too simple to be understood. How the authors set the temperature increment to 2 degrees? Only stations over the TP or all grids in the domain of the TP? please clarify this issue.

Response: We have added the detailed description of the 2°C increment settings. In the sensitivity simulation, we set the 2°C increment at all grids in the domain of the TP. The text is "*According to the meteorological records at weather stations, surface air temperature risen by an average of 2°C from 2013 to 2017 over the Tibetan Plateau (Table S1). ERA-interim reanalysis data also show that the troposphere (600hPa - 250hPa) over the plateau is warming during the 2013-2017 period, and the temperature increment shows a parabolic pattern with the altitude, by an average increase of ~2°C (Figure S1). Thus, we design a sensitivity simulation, with a temperature increase of 2°C in the troposphere over the plateau. In the model, we set to the 2°C warming at all grids covering the plateau (the region surrounded by the dark line in Figure 1b) in the initial and boundary fields. In order to ensure a persistent influence of the 2°C warming, we drive the initial field with a 2°C increment every day. Then, by comparing the difference between the sensitivity simulation and the baseline simulation, we determine the impact of the 2°C warming over the Tibetan Plateau on air quality in the Sichuan Basin.*" In

Lines 167 - 178.

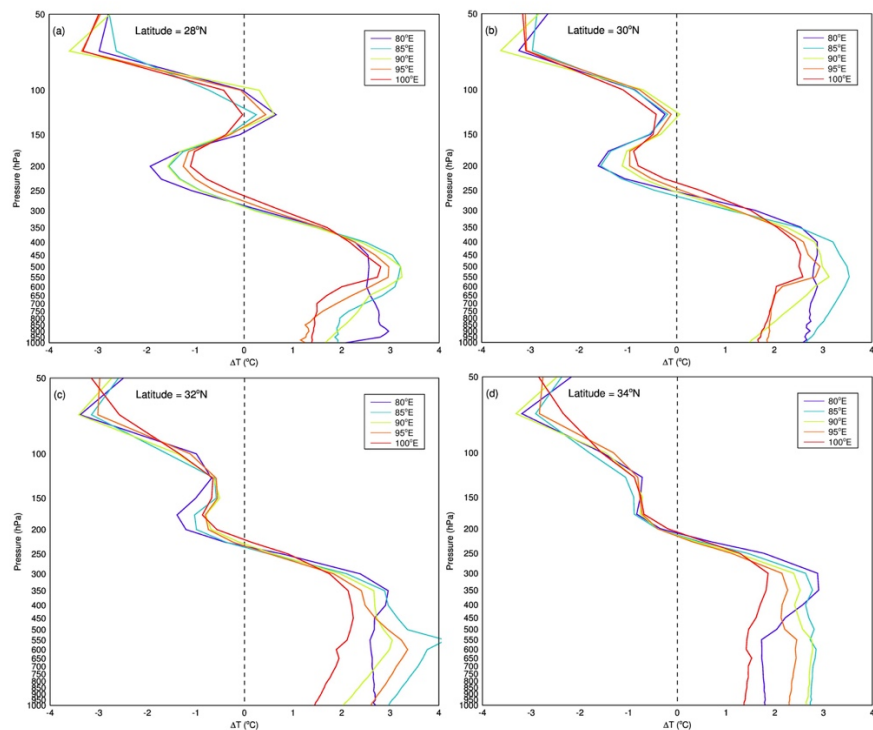


Figure S1 Vertical profile of temperature change along the longitude (80°E - 100°E) covering the plateau at 28°N, 30°N, 32°N and 34°N, ΔT is calculated by the annual temperature increase rate from 2013 to 2017 multiplying by the number of years ($N = 5$). Noted that the temperature in the troposphere over the Tibetan Plateau (600 hPa - 250 hPa) is inhomogeneously warming by 0 - 4 °C from 2013 to 2017, and we take an average warming increase of 2 °C.

Comment 2. Please clarify the mechanism that the warming TP causes less air pollution in the Sichuan Basin. Please make sure whether the warming TP influence large-scale atmospheric circulation through air-land interaction? I think that the warming TP is a result other than a cause.

Response: We have added the analysis of pressure gradient to explain the mechanism between the warming TP and less air pollution in the Sichuan Basin (Figure 8, a new figure). In our study, we focus on how the warming TP affects air pollution via changing winds, temperature and the PBL height as well as RH in the Sichuan Basin.

The text is as follows: “*We further compare the difference in the surface pressure between the baseline and sensitivity simulations, and find out that surface pressure over the plateau and the basin all decreases when the plateau warms by 2°C (Figure 8a and 8b). Over the plateau, the pressure drop has a decrease characteristic from west to east (Figure 8c), which results in a decreased pressure gradient and a weakened westerly wind. While in the basin, the pressure drop is less than the plateau. This leads to an increased pressure gradient from the basin to*

the plateau, inducing an intensified easterly wind. The enhanced easterly wind causes an increased transport of PM_{2.5} from the basin to the plateau. On the other hand, the weakened westerly wind and the enhanced easterly wind are convergent at the border between the plateau and the basin (Figure 7), jointly leading to an increase in PM_{2.5} concentration at the eastern edge of the plateau.” in Lines 279 - 289.

“After the 2°C warming, surface pressure decreases in the basin (Figure 8), which produces more convergent airflow (as shown in Figure 7). The strengthened convergent airflow induces an intensified ascending motion, conducive to a reduction of temperature in the basin. As a result, the zone where the maximal temperature drop appears, overlaps with the zone with the maximal ascending motion. Furthermore, the intensified updraft increases the vertical temperature gradient and the instability in the lower troposphere of the basin, thereby causing a higher PBL height than that in the non-warming case (Figure 10b). On the contrary, the change in vertical temperature profile leads to a decreased vertical temperature gradient and increased thermal stability in the lower troposphere of the plateau, in which the PBL height decreases.

On the other hand, the convergent airflows by a weakened westerly wind over the plateau and a strengthened easterly wind in the basin (shown in Figure 8) triggers an ascending motion on the east side of the plateau, which is also beneficial to the development of the PBL height in the basin. Consequently, the elevated PBL facilitates vertical diffusion, leading to a reduction in PM_{2.5} concentration over the basin.” in Lines 318 - 332.

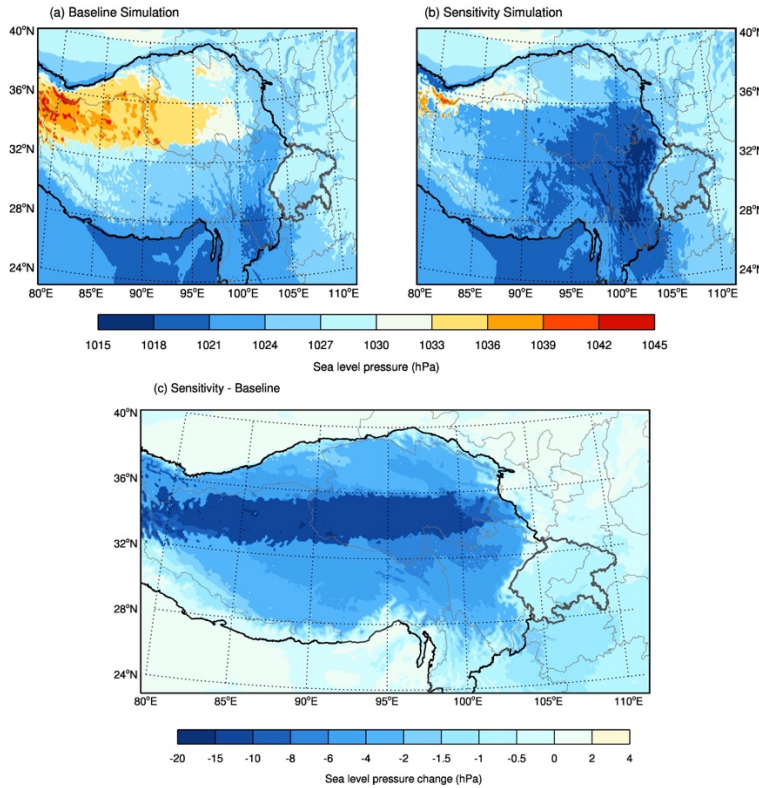


Figure 8 Comparison of spatial distributions of sea level pressure (SLP) between the (a) baseline simulation and (b) sensitivity simulation over the Tibetan Plateau and Sichuan Basin. (c) The SLPs over the plateau and basin decrease while the plateau becomes 2°C warming.

Comment 3. significance testing is important for your results. Please make some significance test for your results. For example, Fig. 5 and Fig. 6 show the difference between observations and simulations. Whether the difference between them is significant?

Response: Thanks for your suggestions, and we have added the Student's *t* test to validate the significant difference between observations and simulations in the revised manuscript. Results show that the difference is extremely significant, and here we have added the *p*-value ($p < 0.001$) in Figure 5, rather than the exact value, because the *p*-value ($p = 5.76E-19$) is far less than 0.001. The related text is “*The results show that PM_{2.5} concentration in the basin is significantly reduced by an average of 25.1 μg m⁻³ in the case of 2°C warming, with a confidence level of 99.9% (p < 0.001).*”

Figure 6 calculates monthly-averaged concentrations of chemical composition in PM_{2.5}. To

calculate the significance of every chemical composition, we use raw data in Figure 5, because $\text{PM}_{2.5}$ concentration is the sum of concentrations of SO_4^{2-} , NO_3^- , NH_4^+ , Cl^- , SOA , POA , EC and Undef in Figure 6. Results show that differences in most of the chemical composition are extremely significant ($p < 0.001$) except that the EC is more significant ($0.001 < p = 0.0011 < 0.01$). The p -values of every chemical composition are summarized as Table S2 in Supplemental materials, not shown in Figure 6. The Table S2 and its related text is below: “*Significance testing of the difference in every chemical composition between the baseline and sensitivity simulations are also given in Table S2. The p-values of most chemical composition in $\text{PM}_{2.5}$ are far less than 0.001 except that the p-value of EC is 0.0011 (Table S2), implying for an extremely significant reduction of every chemical composition in $\text{PM}_{2.5}$ within the basin when the plateau warms by 2°C.*”

Table S2 Significance differences in concentrations of chemical composition in $\text{PM}_{2.5}$ between the baseline simulation and sensitivity simulation. The p -value of every chemical composition is followed.

Chemical composition	SO_4^{2-}	NO_3^-	NH_4^+	Cl^-	SOA	POA	EC	Undef
p -value	2.78E-04	5.05E-06	6.84E-05	3.29E-04	6E-130	2.14E-06	0.0011	2.63E-15

Minor comments:

Comment 4: Fig. 7, please indicate the information of winds.

Response: Added. “*On the other hand, the weakened westerly wind and the enhanced easterly wind are convergent at the border between the plateau and the basin (Figure 7), jointly leading to an increase in $\text{PM}_{2.5}$ concentration at the eastern edge of the plateau. Additionally, northerly winds over the basin slightly enhance, conducive to diluting the air and reducing $\text{PM}_{2.5}$ concentration.*” In Lines 286 - 290.

1 **The Warming Tibetan Plateau improves winter air quality in the Sichuan Basin, China**

2

3 Shuyu Zhao¹, Tian Feng², Xuexi Tie^{1,3*}, Zebin Wang⁴

4

5 ¹Key Laboratory of Aerosol Chemistry and Physics, SKLLQG, Institute of Earth Environment,
6 Chinese Academy of Sciences, Xi'an, 710061, China

7 ²Department of Geography & Spatial Information Techniques, Ningbo University, Ningbo, 315211,
8 China

9 ³Center for Excellence in Urban Atmospheric Environment, Institute of Urban Environment,
10 Chinese Academy of Sciences, Xiamen, 361021, China

11 ⁴Northwest Air Traffic Management Bureau, Civil Aviation Administration of China, Xi'an, 712000,
12 China

13

14 Corresponding author: tiexx@ieecas.cn

15

16 **Key points**

17

18 The Tibetan Plateau is rapidly warming, and the temperature has risen by 2 ° C from 2013 to 2017.

19

20 The 2 ° C warming of the plateau leads to an increase in PBL height and a decrease in humidity in
21 the Sichuan Basin.

22

23 The 2 ° C warming reduces PM_{2.5} concentration in the basin by 25.1 $\mu\text{g m}^{-3}$, of which primary and
24 secondary aerosols are 5.4 $\mu\text{g m}^{-3}$ and 19.7 $\mu\text{g m}^{-3}$, respectively.

25 **Abstract**

26

27 Impacts of global climate change on the occurrence and development of air pollution have attracted
28 more attentions. This study investigates impacts of the warming Tibetan Plateau on air quality in
29 the Sichuan Basin. Meteorological observations and ERA-interim reanalysis data reveal that the
30 Tibetan Plateau has been rapidly warming during the last 40 years (1979-2017), particularly in
31 winter when the warming rate is approximately twice as much as the annual warming rate. Since
32 2013, the winter temperature over the plateau has even risen by 2 ° C. Here, we use the WRF-CHEM
33 model to assess the impact of the 2 ° C warming on air quality in the Sichuan Basin. The model
34 results show that the 2 ° C warming causes an increase in the Planetary Boundary Layer (PBL)
35 height and a decrease in the relative humidity (RH) in the basin. The elevated PBL height
36 strengthens vertical diffusion of PM_{2.5}, while the decreased RH significantly reduces secondary
37 aerosol formation. Overall, PM_{2.5} concentration is reduced by 17.5% (~25.1 $\mu\text{g m}^{-3}$), of which the
38 reduction in primary and secondary aerosols is 5.4 $\mu\text{g m}^{-3}$ and 19.7 $\mu\text{g m}^{-3}$, respectively. These
39 results reveal that the recent warming plateau has improved air quality in the basin, to some certain
40 extent, mitigating the air pollution therein. Nevertheless, climate system is particularly complicated,
41 and more studies are needed to demonstrate the impact of climate change on air quality in the
42 downstream regions as the plateau is likely to continue warming.

43

44 **Keywords:** climate change, air quality, Tibetan Plateau, WRF-CHEM model

45

46 **1 Introduction**

47

48 The Tibetan Plateau is known as the third pole because of its high altitude and large area. It is also
49 regarded as an important response region to the Northern Hemisphere, and even global climate due
50 to its sensitivity to climate change. Previous studies on the Tibetan Plateau show that the region was
51 experiencing warming in the second half of the 20th century, especially in the winter months (Kuang
52 and Jiao, 2016; Liu and Chen, 2000; Rangwala et al., 2009). The warming plateau not only plays a
53 significant role in driving the weather and climate change, as well as the ecological system, but also
54 has an important impact on air quality in the downstream regions. Xu et al. (2016) suggest that the
55 thermal anomaly over the Tibetan Plateau obviously increases haze frequency and surface aerosol
56 concentration in central-eastern China.

57

58 However, the impacts of climate change on air quality in China are still unclear. Some researches
59 hold the opinion that climate change induced by greenhouse gas emission increases severe haze
60 occurrence and intensity in winter at Beijing, and its impact will continue in the future (Cai et al.,
61 2017; Zou et al., 2017). Similarly, Xu et al. (2017) suggest that climate warming anomaly in the
62 lower and middle troposphere over the continent around the Yangtze River Delta leads to more haze
63 days in winter during recent decades. On the contrary, another opinion suggests that climate change
64 in the past two decades is favorable for air pollution dispersion in northern China via enhancing
65 mid-latitude cold surges in winter (Zhao et al., 2018). If cold surge is strong enough, pollutants
66 would be transported to the downstream regions, causing a better air quality in the upstream region
67 but a worse one in the downstream region. Thus, there may be regional differences in the impact of
68 climate change on air quality.

69

70 Previous studies on air pollution in China are concentrated in the developed regions, such as the
71 North China Plain, the Yangtze River Delta and the Pearl River Delta. Few studies have paid
72 attention to the Sichuan Basin, although the region is undergoing severe air pollution, and mean
73 PM_{2.5} concentration is more than 110 $\mu\text{g m}^{-3}$ in winter (Qiao et al., 2019; Tao et al., 2017; Wang et

74 al., 2018; Yang et al., 2011). Thus, it is necessary to explore the underlying causes that leads to air
75 pollution in the Sichuan Basin.

76
77 The Sichuan Basin locates in the downstream region of the Tibetan Plateau, and its weather
78 conditions are obviously affected by the plateau (Duan et al., 2012; Hua, 2017; Zhao et al., 2019).
79 For instance, the foggy weather, southwest vortex and low-level shear line over the basin are closely
80 associated with the plateau (Zhu et al., 2000). These changes in weather conditions induced by the
81 plateau undoubtedly affect the development and dispersion of air pollution in the basin, because the
82 huge terrain can trigger a thermodynamic forcing, which is of great importance for weather
83 conditions in the surrounding regions (Bei et al., 2016; 2017; Zhao et al., 2015).

84
85 This study therefore focuses on how climate change on the Tibetan Plateau affects air quality in the
86 Sichuan Basin in recent years. Section 3 analyzes the climate change on the Tibetan Plateau in the
87 past four decades, and especially emphasizes the change in recent five years. In Section 4, we design
88 two numerical simulations to calculate the impact of climate change on air quality. One is a baseline
89 simulation, which is constrained by observed surface meteorological parameters and pollutant
90 concentrations. The other is a sensitivity simulation, which uses the same emission inventory and
91 meteorological fields as the baseline simulation except for the changed air temperature. We compare
92 the difference of PM_{2.5} concentrations in these two cases, and also calculate the differences in
93 meteorological parameters that include winds (wind speed and direction), air temperature, and
94 relative humidity (RH), as well as the Planetary Boundary Layer (PBL) height. Based on the
95 differences in PM_{2.5} concentration and meteorological parameters above, we finally explain the
96 cause-to-effect relationship between climate change on the Tibetan Plateau and the changes in the
97 PBL height and RH in the Sichuan Basin. Moreover, we calculate the effect of the relationship on
98 air quality in the Sichuan Basin.

99
100 **2 Data and Methods**

101

102 **2.1 Observations**

103

104 To ensure a robust result, we use two datasets of surface air temperature in this study. One is the
105 European Center for Medium-Range Weather Forecasts (ECMWF) ERA-Interim monthly mean
106 reanalysis data (1979-2018), obtained from the website of <http://apps.ecmwf.int/datasets/>, with the
107 finest horizontal resolution of $0.125^\circ \times 0.125^\circ$. The other is hourly and monthly mean weather-station
108 observations from the National Oceanic and Atmospheric Administration (NOAA), which is
109 available on the website of
110 <http://gis.ncdc.noaa.gov/map/viewer/#app=clim&cfg=ledo&theme=hourly&layers=1&node=gis>.

111

112 Figure 1 shows the distribution of weather stations over the Tibetan Plateau, and these weather
113 stations widely cover the entire plateau. Trends of annual mean and winter surface air temperature
114 over the plateau are analyzed, and the winter is averaged over 3-month periods (December-January-
115 February). Additionally, we use ambient air quality data to validate the model performance. Since
116 2013, the data are released by Ministry of Environmental Protection, China at
117 <http://www.aqistudy.cn/>, including hourly PM_{2.5}, CO, and O₃ mass concentrations. The monitoring
118 stations for air quality are also shown in Figure 1.

119

120 **2.2 Model configuration and experiments**

121

122 A state-of-the-art regional dynamical and chemical model (WRF-CHEM model) is used in the
123 study. The simulation domain covers the Tibetan Plateau and the Sichuan Basin (Figure 1). The
124 Tibetan Plateau covers about 2.5 million km², with the averaged elevation of 4500 m, and the
125 Sichuan Basin covers about 0.16 million km², with the elevation in the center of the basin less than
126 1000 m (250 - 700 m). The model is set by a horizontal grid resolution of 9 km (451 × 221 grids),
127 with 35 vertical sigma levels. The model description in detail is seen by Grell et al. (2005). The
128 evaluation of the model performance has been conducted by many previous studies (Li et al., 2011a;
129 Tie et al., 2009; 2007). In this study, we use the Goddard longwave and shortwave radiation

130 parameterization (Dudhia, 1989), the WSM 6-class graupel microphysics scheme (Hong and Lim,
131 2006), the Mellor-Yamada-Janji (MYJ) planetary boundary layer scheme (Janjić, 2002), the unified
132 Noah land-surface model (Chen and Dudhia, 2001) and Monin-Obukhov surface layer scheme
133 (Janjić, 2002). For chemical schemes, we use a new flexible gas-phase chemical module and the
134 Community Multiscale Air Quality (CMAQ, version 4.6) aerosol module developed by the US
135 EPA (Binkowski, 2003). Gas-phase atmospheric reactions of volatile organic compounds (VOCs)
136 and nitrogen oxide (NO_x) use the SAPRC-99 (Statewide Air Pollution Research Center, version
137 1999) chemical mechanism. Inorganic aerosols use the ISORROPIA version 1.7, referring to Li et
138 al. (2011a) and Feng et al. (2016). A SO₂ heterogeneous reaction mechanism on aerosol surfaces
139 involving aerosol water is added (Li et al., 2017a), and NO₂ heterogeneous reaction to produce
140 HONO is also considered (Li et al., 2010). The secondary organic aerosol (SOA) calculation uses
141 a non-traditional volatility basis-set approach by Li et al. (2011b). The photolysis rates are
142 calculated by a fast Tropospheric Ultraviolet and Visible (FTUV) radiation transfer model, in which
143 the impacts of aerosols and clouds on the photochemistry processes are considered (Li et al., 2011a;
144 Tie et al., 2003; 2005). The wet deposition is calculated by the method used in CMAQ and the dry
145 deposition follows Wesely (1989).

146

147 We use the MIX anthropogenic emission inventory for the year of 2010, and it is available at Multi-
148 resolution Emission Inventory for China (<http://www.meicmodel.org/dataset-mix.html>), consisting
149 of industrial, power, transportation, and agricultural as well as residential sources (Li et al., 2017b;
150 Zhang et al., 2009). **The emission inventory is constructed by a ‘bottom-up’ approach based on**
151 **national and provincial activity data and emission factors. To improve the emission inventory**
152 **accuracy, we use a ‘top-down’ method here to constrain the emission inventory. We compare the**
153 **simulated value with the measured value time and again until the simulations are close to the**
154 **measurements.** The biogenic emissions are online calculated by the Model of Emissions of Gases
155 and Aerosol from Nature (MEGAN) (Guenther et al., 2006). Initial and boundary meteorological
156 fields in the model are driven by 6-hour 1° × 1° NCEP (National Centers for Environmental
157 Prediction) reanalysis data. Chemical lateral conditions are provided by a global chemistry

158 transport model – MOZART (Model for OZone And Related chemical Tracer, version 4), with a 6-
159 h output (Emmons et al., 2010; Tie et al., 2005). The spin-up time of the WRF-CHEM model is 1
160 day.

161

162 Two numerical experiments are performed. One is the baseline simulation in the 2013-2014 winter
163 (January 2014), and the other is a sensitivity simulation that has an observational increase in air
164 temperature over the Tibetan Plateau. In other words, the sensitivity simulation uses the same
165 emission inventory and meteorological conditions as the baseline simulation except that the
166 temperature fields over the Tibetan Plateau are changed. According to the meteorological records
167 at weather stations, surface air temperature risen by an average of 2°C from 2013 to 2017 over the
168 Tibetan Plateau (Table S1). ERA-interim reanalysis data also show that the troposphere (600hPa -
169 250hPa) over the plateau is warming during the 2013-2017 period, and the temperature increment
170 shows a parabolic pattern with the altitude, by an average increase of ~2°C (Figure S1). Thus, we
171 design a sensitivity simulation, with a temperature increase of 2°C in the troposphere over the
172 plateau. In the model, we set to the 2°C warming at all grids covering the plateau (the region
173 surrounded by the dark line in Figure 1b) in the initial and boundary fields. In order to ensure a
174 persistent influence of the 2°C warming, we drive the initial field with a 2°C increment every day.
175 Then, by comparing the difference between the sensitivity simulation and the baseline simulation,
176 we determine the impact of the 2°C warming over the Tibetan Plateau on air quality in the Sichuan
177 Basin.

178

179 **3 The warming Tibetan Plateau in the last four decades**

180

181 Figure 2 shows the variability and linear trend of surface air temperature at 10 weather stations
182 over the Tibetan Plateau in winter during the last four decades (1979 - 2017). The winter mean
183 temperature recorded from all the weather stations exhibits an obvious annual fluctuation and the
184 linear regression shows a significant rising trend. Clearly, the plateau is continuously undergoing
185 a warming phase, albeit with regional differences in the warming magnitude. The warming rates in

186 different regions vary in the range of 0.5 - 1.0°C decade⁻¹. Compared with the warming rate of
187 annual mean temperature (Figure S1), the warming rate in winter is approximately twice as much,
188 suggesting that the warming in winter is more significant.

189

190 Using the ERA-interim reanalysis data, Figure 3 shows the temperature change during the same
191 period (1979 - 2017). The result is consistent with weather records, showing that air temperature
192 is significantly rising in most parts of the plateau. The maximal warming rate is around 0.6 - 0.8°C
193 decade⁻¹, appeared in the central and southern plateau. The warming in the rest areas is slighter,
194 with a rate of 0.3 - 0.6 °C decade⁻¹. Particularly, the averaged warming rate in the vast central
195 plateau reaches about 1.0°C yr⁻¹ in recent five years (Figure S2), greater than the warming rate
196 during the entire 40 years (Figure 3). Both the observation records and reanalysis data evidently
197 show that the plateau has been warming in the last four decades, and also the warming trend for
198 recent years is more significant.

199

200 From the above temperature change analysis, we notice that there is obviously a positive
201 temperature anomaly between 2013 and 2017 winters, implying for an accelerating warming over
202 the plateau. The observational temperature in winter increases by about 2°C between 2013 and
203 2017. Therefore, the impact of the 2°C warming on air quality in the Sichuan Basin is investigated.
204 In order to isolatedly assess the effect of a rapid temperature increase and to eliminate the effect of
205 other factors, a sensitivity study using the WRF-CHEM model is conducted for considering the
206 2°C temperature increase from the value in 2013 (see Figure 2 and Table S1).

207

208 **4 Results and Discussion**

209

210 **4.1 Model validation**

211

212 To systemically evaluate the model performance on simulation O₃, CO and PM_{2.5} mass
213 concentrations, three statistical indices are used. They are the mean bias (MB), root mean square

214 error (RMSE), and index of agreement (IOA). The calculation formulas are given in Text S1. The
215 IOAs of air temperature and RH are 0.85 and 0.79, respectively (Figure S3), suggesting that the
216 model well captures the diurnal cycle of temperature and the variability of RH. However, the
217 calculated wind speed is overestimated, especially in the region between the Tibetan Plateau and
218 the Sichuan Basin. This is because there is a dramatic elevation drop in the region, which makes it
219 difficult for the model to replicate the observed wind speed and direction.

220

221 Figure 4 shows comparisons of hourly O₃, CO and PM_{2.5} concentrations between the model
222 simulations and measurements. The result shows that the simulated CO mean level is close to the
223 measurement, with a MB of 0.11 mg m⁻³, indicating that the model reasonably reproduces the
224 meteorological fields and long-range transport. Because the chemical lifetime of CO is relatively
225 long (~months), the variability of CO is dominantly determined by the meteorological fields and
226 atmospheric transport process. For the simulation of O₃, in addition to the effects of meteorological
227 fields and atmospheric transport process, its variability is strongly controlled by the photochemical
228 process. The model result shows that the simulated diurnal cycle of O₃ is reasonably agreed with
229 the measurement, with an IOA of 0.79. There is only a small bias between the simulated and
230 measured O₃ mean concentration. The simulated O₃ concentration is 1.7 $\mu\text{g m}^{-3}$ higher than the
231 measurement, suggesting that both the photochemistry and long-range transport well capture the O₃
232 variability in the region. Finally, the IOA between the simulated and measured PM_{2.5} concentrations
233 is 0.80, indicating that the aerosol module in the model generally captures the measured PM_{2.5}
234 variation.

235

236 However, there are some noticeable discrepancies between the simulations and the measurements.
237 For instance, the simulated magnitude of PM_{2.5} concentration is larger than the measurement, and
238 its mean level is underestimated by 13.1 $\mu\text{g m}^{-3}$, less than 10% of the measurement (~153.5 $\mu\text{g m}^{-3}$).
239 These discrepancies are likely due to the biases in the uncertainties in emission inventory and
240 small-scale dynamical fields. During the period of Jan 17th to Jan 20th, the observed wind speed
241 concentrates in the range of 1 - 2 m s⁻¹, with an average of 1.3 m s⁻¹, while the simulated wind speed

242 is obviously higher, with an average of 2.0 m s^{-1} (Figure S3). The observed prevailing wind is
243 northerly wind while the simulated prevails easterly wind. Figure S6a shows that $\text{PM}_{2.5}$
244 concentration is lower in the north to the Sichuan Basin while higher to in the east to the basin.
245 Therefore, the overestimated $\text{PM}_{2.5}$ concentration is mainly caused by the departure of winds, which
246 results in a false transport from the east to the basin. This is also shown by the overestimation of
247 CO concentration because the observed northerly wind is not well simulated due to the complicated
248 topography.

249

250 **4.2 Change in winter $\text{PM}_{2.5}$ concentration over the basin**

251

252 To examine impacts of the warming plateau on $\text{PM}_{2.5}$ concentration in winter in the Sichuan Basin,
253 the time series of $\text{PM}_{2.5}$ concentrations in the two case simulations (i.e., with and without the 2°C
254 warming over the plateau) are respectively calculated (Figure 5). The results show that $\text{PM}_{2.5}$
255 concentration in the basin is significantly reduced by an average of $25.1 \mu\text{g m}^{-3}$ in the case of 2°C
256 warming, with a confidence level of 99.9% ($p < 0.001$). The maximum hourly reduction reaches to
257 $84.6 \mu\text{g m}^{-3}$ (Figure S4a) and the maximum percentage reduction is about 64.5% (Figure S4b).
258 Interestingly, the maximum reduction always occurs while $\text{PM}_{2.5}$ concentration reaches a peak
259 value, which suggests that the impact of the warming plateau is extremely significant during the
260 period of high $\text{PM}_{2.5}$ concentration. This result is similar to previous studies which also point out
261 that extreme weather plays important roles in affecting air quality (De Sario et al., 2013; Hong et
262 al., 2019; Tsangari et al., 2016; Zhang et al., 2016). That is to say, the impact of the warming plateau
263 on air quality is apt to be amplified in extremely high $\text{PM}_{2.5}$ concentrations.

264

265 To better understand the impact of the warming plateau on $\text{PM}_{2.5}$ concentration in the Sichuan
266 Basin, we also calculate the changes in $\text{PM}_{2.5}$ chemical composition in the basin (Figure 6). As a
267 result, secondary aerosol reduces by $19.7 \mu\text{g m}^{-3}$, accounting for 78.5% of the total reduction. For
268 example, the largest reduction is SOA, reducing from $23.2 \mu\text{g m}^{-3}$ in the base case to $10.8 \mu\text{g m}^{-3}$
269 in the warming case. The second reduction is sulfate ($31.8 \mu\text{g m}^{-3}$ in the base case and $28.6 \mu\text{g m}^{-3}$

270 in the warming case). The next are nitrate and ammonium ($22.3 \mu\text{g m}^{-3}$ and $19.1 \mu\text{g m}^{-3}$ in the base
271 case, and $20.2 \mu\text{g m}^{-3}$ and $17.5 \mu\text{g m}^{-3}$ in the warming case). **Significance testing of the difference**
272 in every chemical composition between the baseline and sensitivity simulations are also given in
273 Table S2. The *p*-values of most chemical composition in $\text{PM}_{2.5}$ are far less than 0.001 except that
274 the *p*-value of EC is 0.0011 (Table S2), implying for an extremely significant reduction of every
275 chemical composition in $\text{PM}_{2.5}$ within the basin when the plateau warms by 2°C .

276

277 There are also significant changes in the spatial distribution of $\text{PM}_{2.5}$ concentration. Figure 7 shows
278 the spatial distribution of changes in surface $\text{PM}_{2.5}$ concentration and winds after 2°C warming over
279 the plateau. Apparently, there is a larger decrease in $\text{PM}_{2.5}$ concentration in the whole basin, and the
280 maximum reduction is more than $30 \mu\text{g m}^{-3}$. By contrast, $\text{PM}_{2.5}$ concentration increases by 5 - 15 μg
281 m^{-3} at the eastern edge of the plateau. **Wind patterns show that easterly winds over the basin enhance**
282 **while westerly wind over the plateau weaken** (Figure S6 and Figure 7). We further compare the
283 difference in the surface pressure between the baseline and sensitivity simulations, and find out that
284 surface pressure over the plateau and the basin all decreases when the plateau warms by 2°C (Figure
285 8a and 8b). Over the plateau, the pressure drop has a decrease characteristic from west to east (Figure
286 8c), which results in a decreased pressure gradient and a weakened westerly wind. While in the
287 basin, the pressure drop is less than the plateau. This leads to an increased pressure gradient from
288 the basin to the plateau, inducing an intensified easterly wind. The enhanced easterly wind causes
289 an increased transport of $\text{PM}_{2.5}$ from the basin to the plateau. On the other hand, the weakened
290 westerly wind and the enhanced easterly wind are convergent at the border between the plateau and
291 the basin (Figure 7), jointly leading to an increase in $\text{PM}_{2.5}$ concentration at the eastern edge of the
292 plateau. Additionally, northerly winds over the basin slightly enhance, conducive to diluting the air
293 and reducing $\text{PM}_{2.5}$ concentration. Both easterly winds transport and northerly winds dilution are
294 favorable for a reduction of $\text{PM}_{2.5}$ concentration in the basin. In addition to the wind effect, there
295 are also other important factors to produce the $\text{PM}_{2.5}$ reduction in the basin, such as the PBL height
296 and RH, which will be analyzed as follows.

297

298 **4.3 Impact of PBL height on PM_{2.5} concentration**

299

300 Previous studies show that the PBL development plays an important role in diffusing pollutants
301 (Miao et al., 2017; Su et al., 2018; Tie et al., 2015). Here we calculate the change in the PBL height
302 due to the 2°C warming over the plateau, and then analyze the effect of the change in PBL height
303 on PM_{2.5} concentration in the basin.

304

305 Our results suggest that the 2°C warming plays different roles in the PBL development over the
306 plateau and the basin. Due to the 2°C warming, the PBL height decreases in most areas of the plateau,
307 but rises by 50 - 200 m over the basin (Figure 9). As known, a shallow PBL constrains PM_{2.5} near
308 the surface via suppressing vertical dispersion (Fan et al., 2011; Iversen, 1984). Conversely, a deep
309 PBL is favorable for PM_{2.5} diffusion. Thus, we explore the underlying cause that leads to the
310 difference in the PBL height over the plateau and the basin. Figure 10 shows that vertical profiles
311 of changes in temperature and winds in the plateau and the basin, because the PBL height is strongly
312 related to the changes in vertical temperature and wind. The results show that the 2°C warming
313 causes a maximum warm layer around 1 km above the ground of the plateau. Interestingly, the warm
314 layer acts as a dome covering 4.5 km above the Sichuan Basin (Figure 10a). Xu et al. (2017) also
315 finds out a significant warm plume extending from the plateau to the downstream Sichuan Basin
316 and Yangtze River Delta by use of NCEP/NCAR reanalysis data. This is probably due to a sharp
317 topography decrease (from ~ 5 km in the plateau to < 1 km in the basin) that leads to a warm plume
318 via subsidence. In the basin, there is a decrease in the temperature from the surface to ~ 4 km, with
319 a maximal temperature reduction (1 - 2°C) located at 1.5 km to 3 km above the ground (Figure 10a).
320 We speculate that changes in the surface pressure can account for the maximal temperature reduction
321 here. After the 2°C warming, surface pressure decreases in the basin (Figure 8), which produces
322 more convergent airflow (as shown in Figure 7). The strengthened convergent airflow induces an
323 intensified ascending motion, conducive to a reduction of temperature in the basin. As a result, the
324 zone where the maximal temperature drop appears, overlaps with the zone with the maximal
325 ascending motion. Furthermore, the intensified updraft increases the vertical temperature gradient

326 and the instability in the lower troposphere of the basin, thereby causing a higher PBL height than
327 that in the non-warming case (Figure 10b). On the contrary, the change in vertical temperature
328 profile leads to a decreased vertical temperature gradient and increased thermal stability in the lower
329 troposphere of the plateau, in which the PBL height decreases.

330

331 On the other hand, the convergent airflows by a weakened westerly wind over the plateau and a
332 strengthened easterly wind in the basin (shown in Figure 8) triggers an ascending motion on the east
333 side of the plateau, which is also beneficial to the development of the PBL height in the basin.
334 Consequently, the elevated PBL facilitates vertical diffusion, leading to a reduction in PM_{2.5}
335 concentration over the basin.

336

337 **4.4 Effect of RH on PM_{2.5} concentration**

338

339 In addition to the PBL height, ambient RH is a key factor for secondary aerosol formation (Tie et
340 al., 2017; Wang et al., 2016). Previous studies indicate that aerosol hygroscopic growth cannot
341 occurs until the humidity exceeds 50% (Liu et al., 2008). When the humidity is greater than 60%,
342 hygroscopic growth factor of urban aerosol increases significantly with humidity (Liu et al., 2008).

343

344 Figure 11 shows that there is remarkable change in RH in the basin due to the 2°C warming of the
345 plateau. In the baseline simulation, the RH varies in the range of 40% - 80% over the basin (Figure
346 11a). However, the RH varies from 40% to 70% in the 2 °C warming simulation (Figure 11b),
347 suggesting that the basin becomes drier when the plateau is warmer.

348

349 The RH comparison between these two numerical simulations reveals that the 2 °C warming causes
350 a 2.5% - 10% decrease in the RH over the basin (Figure 11c). This change in RH has a critical effect
351 on the secondary aerosol formation. As explained by Tie et al. (2017), the reduction of RH
352 (especially during the stage of RH from 80% to 70%) causes a significant decrease of hygroscopic
353 growth on the aerosol surface, resulting in less water surface for producing secondary aerosol, such
354 as sulfate and nitrate. As a result, the PM_{2.5} concentration decreases in the basin. There are also some

355 fingerprints of the RH's effect on $\text{PM}_{2.5}$ concentration. Firstly, the spatial distributions of RH
356 reduction and $\text{PM}_{2.5}$ concentration reduction have similar patterns (Figure 11c and Figure 7), and
357 the region with more humidity decrease overlaps the region with more $\text{PM}_{2.5}$ decreases. Secondly,
358 as shown in Figure 6, the changes in $\text{PM}_{2.5}$ compositions indicate that the reduced $\text{PM}_{2.5}$
359 concentration is mainly caused by the decrease in secondary aerosol concentration. Therefore, the
360 RH change plays an important role for $\text{PM}_{2.5}$ concentration in the basin.

361

362 **5 Conclusions**

363

364 ERA-interim reanalysis data and observation records at 10 weather stations show that the Tibetan
365 Plateau is significantly warming during the past four decades (1979-2017), particularly in winter.
366 The temperature increase rate is $0.5^{\circ}\text{C decade}^{-1}$ to $1.0^{\circ}\text{C decade}^{-1}$ in winter, approximately twice as
367 much as the increase rate of annual mean temperature. In recent 5 years (2013-2017), the central
368 plateau is significantly warming with an increase rate of $1.0^{\circ}\text{C yr}^{-1}$, encompassing the warming rate
369 during the entire 40 years. Rapid warming has caused the winter temperature to increase by an
370 average of 2°C over the entire plateau from 2013 to 2017.

371

372 The WRF-Chem model is used to assess the impact of 2°C warming of the plateau on air quality
373 over the downstream Sichuan Basin. The most significant impact of the 2°C warming on $\text{PM}_{2.5}$
374 concentration in the basin is via reducing relative humidity and increasing PBL height. A lower
375 ambient humidity decreases aerosol hygroscopic growth, which weakens secondary aerosol
376 formation and leads to a significant reduction in secondary aerosol concentration. Moreover, the
377 2°C warming induces an increase in vertical temperature gradient over the basin, strengthening
378 turbulence mixing and elevating PBL height. The elevated PBL height is favorable for vertical
379 diffusion that causes a reduction of $\text{PM}_{2.5}$ in the basin. Additionally, the uplift effect by an enhanced
380 ascending motion at the eastern edge of the plateau also contributes to $\text{PM}_{2.5}$ reduction within the
381 basin.

382

383 In summary, the 2°C warming over the plateau in recent five years comprehensively induces a rising
384 PBL height and a drying ambient air over the basin, which greatly reduces PM_{2.5} secondary
385 compositions. On average, PM_{2.5} concentration reduces by 25.1 $\mu\text{g m}^{-3}$, of which the primary and
386 secondary aerosols decrease by 5.4 $\mu\text{g m}^{-3}$ and 19.7 $\mu\text{g m}^{-3}$, respectively. Since the plateau is likely
387 to continue warming, in-depth understanding to climate change on the Tibetan Plateau is required.
388 Long-term PM_{2.5} monitoring is also needed to validate the impact of the warming plateau on air
389 quality.

390

391 *Data availability.* The data used in this study are available from the corresponding author upon
392 request (tiexx@ieecas.cn).

393 *Supplement.* Supplemental materials to this article can be found online at <http://xxxxxx>

394 *Author contributions.* XX designed research, and revised the final paper. SY performed research,
395 and wrote the paper. XX and SY provided financial support. TF validated the model, modified the
396 chart code and reviewed the paper. ZB collected and analyzed the weather-stations data.

397 *Competing interests.* The authors declare that they have no conflict of interest.

398 *Acknowledgements.* This work is supported by the National Natural Science Foundation of China
399 (Nos. 41430424, 41730108 and 41807307) and the West Light Foundation of the Chinese Academy
400 of Sciences (Nos. XAB2016B04). We also would like to acknowledge European Center for
401 Medium-Range Weather Forecasts (ERA-interim) for reanalysis data which are freely obtained by
402 a following registration on the website <http://apps.ecmwf.int/datasets/>. Ambient weather-station
403 observations are obtained from the National Oceanic and Atmospheric Administration (NOAA),
404 <http://gis.ncdc.noaa.gov/map/viewer/#app=clim&cfg=ledo&theme=hourly&layers=1&node=gis>.
405 The hourly ambient surface O₃, CO and PM_{2.5} mass concentrations are real-timely released by
406 Ministry of Environmental Protection, China on the website <http://www.aqistudy.cn/>, freely
407 downloaded from <http://106.37.208.233:20035/>. The MEIC-2012 (Multi-resolution Emission
408 Inventory for China) anthropogenic emission inventory is available on the website,
409 <http://www.meicmodel.org>. The authors also thank anonymous reviewers for their helpful
410 comments and suggestions.

411 **Reference**

412 Bei, N., Li, G., Huang, R.-J., Cao, J., Meng, N., Feng, T., Liu, S., Zhang, T., Zhang, Q. and Molina,
413 L. T.: Typical synoptic situations and their impacts on the wintertime air pollution in the Guanzhong
414 basin, China, *Atmos. Chem. Phys.*, 16(11), 7373–7387, doi:10.5194/acp-16-7373-2016, 2016.

415 Bei, N., Zhao, L., Xiao, B., Meng, N. and Feng, T.: Impacts of local circulations on the wintertime
416 air pollution in the Guanzhong Basin, China, *Science of The Total Environment*, 592, 373–390,
417 doi:10.1016/j.scitotenv.2017.02.151, 2017.

418 Binkowski, F. S.: Models-3 Community Multiscale Air Quality (CMAQ) model aerosol component
419 1. Model description, *J. Geophys. Res.*, 108(D6), 2981, doi:10.1029/2001JD001409, 2003.

420 Cai, W., Li, K., Liao, H., Wang, H. and Wu, L.: Weather conditions conducive to Beijing severe
421 haze more frequent under climate change, *Nat. Clim. Change*, 7(4), 257–262,
422 doi:10.1038/nclimate3249, 2017.

423 Chen, F. and Dudhia, J.: Coupling an Advanced Land Surface–Hydrology Model with the Penn
424 State–NCAR MM5 Modeling System. Part I: Model Implementation and Sensitivity, *Mon. Weather
425 Rev.*, 129(4), 569–585, doi:10.1175/1520-0493(2001)129<0569:CAALSH>2.0.CO;2, 2001.

426 De Sario, M., Katsouyanni, K. and Michelozzi, P.: Climate change, extreme weather events, air
427 pollution and respiratory health in Europe, *Eur Respir J*, 42(3), 826–843,
428 doi:10.1183/09031936.00074712, 2013.

429 Duan, A., Wu, G., Liu, Y., Ma, Y. and Zhao, P.: Weather and climate effects of the Tibetan Plateau,
430 *Adv. in Atmos. Sci.*, 29(5), 978–992, doi:10.1007/s00376-012-1220-y, 2012.

431 Dudhia, J.: Numerical Study of Convection Observed during the Winter Monsoon Experiment
432 Using a Mesoscale Two-Dimensional Model, *J. Atmos. Sci.*, 46(20), 3077–3107, doi:10.1175/1520-
433 0469(1989)046<3077:NSOCOD>2.0.CO;2, 1989.

434 Emmons, L. K., Walters, S., Hess, P. G., Lamarque, J. F., Pfister, G. G., Fillmore, D., Granier, C.,
435 Guenther, A., Kinnison, D., Laepple, T., Orlando, J., Tie, X., Tyndall, G., Wiedinmyer, C.,
436 Baughcum, S. L. and Kloster, S.: Description and evaluation of the Model for Ozone and Related
437 chemical Tracers, version 4 (MOZART-4), *Geosci. Model Dev.*, 3(1), 43–67, doi:10.5194/gmd-3-
438 43-2010, 2010.

439 Fan, S. J., Fan, Q., Yu, W., Luo, X. Y., Wang, B. M., Song, L. L. and Leong, K. L.: Atmospheric
440 boundary layer characteristics over the Pearl River Delta, China, during the summer of 2006:
441 measurement and model results, *Atmos. Chem. Phys.*, 11(13), 6297–6310, doi:10.5194/acp-11-
442 6297-2011, 2011.

443 Feng, T., Li, G., Cao, J., Bei, N., Shen, Z., Zhou, W., Liu, S., Zhang, T., Wang, Y., Huang, R.-J., Tie,
444 X. and Molina, L. T.: Simulations of organic aerosol concentrations during springtime in the
445 Guanzhong Basin, China, *Atmos. Chem. Phys.*, 16(15), 10045–10061, doi:10.5194/acp-16-10045-
446 2016, 2016.

447 Grell, G. A., Peckham, S. E., Schmitz, R., McKeen, S. A., Frost, G., Skamarock, W. C. and Eder,
448 B.: Fully coupled “online” chemistry within the WRF model, *Atmos. Environ.*, 39(37), 6957–6975,
449 doi:10.1016/j.atmosenv.2005.04.027, 2005.

450 Guenther, A., Karl, T., Harley, P., Wiedinmyer, C., Palmer, P. I. and Geron, C.: Estimates of global
451 terrestrial isoprene emissions using MEGAN (Model of Emissions of Gases and Aerosols from
452 Nature), *Atmos. Chem. Phys.*, 6(11), 3181–3210, doi:10.5194/acp-6-3181-2006, 2006.

453 Hong, C., Zhang, Q., Zhang, Y., Davis, S. J., Tong, D., Zheng, Y., Liu, Z., Guan, D., He, K. and
454 Schellnhuber, H. J.: Impacts of climate change on future air quality and human health in China, *P.*
455 *Natl. Acad. Sci. USA*, 116(35), 17193–17200, doi:10.1073/pnas.1812881116, 2019.

456 Hong, S.-Y. and Lim, J.-O. J.: The WRF single-moment 6-class microphysics scheme (WSM6), *J.*
457 *Korean Meteor. Soc.*, 42(2), 129–151, 2006.

458 Hua, M.: Analysis and simulation study on the influence of heat condition over Qinghai-Xizang
459 Plateau on climate over South-West China, *Plateau Meteorology*, 22, 152–156, 2017.

460 Iversen, T.: On the atmospheric transport of pollution to the Arctic, *Geophys. Res. Lett.*, 11(5), 457–
461 460, doi:10.1029/GL011i005p00457, 1984.

462 Janjić, Z. I.: Nonsingular implementation of the Mellor-Yamada level 2.5 scheme in the NCEP meso
463 model, Camp Springs, MD. 2002.

464 Kuang, X. and Jiao, J. J.: Review on climate change on the Tibetan Plateau during the last half
465 century, *J. Geophys. Res.*, 1–29, doi:10.1002/(ISSN)2169-8996, 2016.

466 Li, G., Bei, N., Cao, J., Huang, R., Wu, J., Feng, T., Wang, Y., Liu, S., Zhang, Q., Tie, X. and Molina,
467 L. T.: A possible pathway for rapid growth of sulfate during haze days in China, *Atmos. Chem. Phys.*,
468 17(5), 3301–3316, doi:10.5194/acp-17-3301-2017, 2017a.

469 Li, G., Bei, N., Tie, X. and Molina, L. T.: Aerosol effects on the photochemistry in Mexico City
470 during MCMA-2006/MILAGRO campaign, *Atmos. Chem. Phys.*, 11(11), 5169–5182,
471 doi:10.5194/acp-11-5169-2011, 2011a.

472 Li, G., Lei, W., Zavala, M., Volkamer, R., Dusanter, S., Stevens, P. and Molina, L. T.: Impacts of
473 HONO sources on the photochemistry in Mexico City during the MCMA-2006/MILAGO
474 Campaign, *Atmos. Chem. Phys.*, 10(14), 6551–6567, doi:10.5194/acp-10-6551-2010, 2010.

475 Li, G., Zavala, M., Lei, W., Tsimpidi, A. P., Karydis, V. A., Pandis, S. N., Canagaratna, M. R. and
476 Molina, L. T.: Simulations of organic aerosol concentrations in Mexico City using the WRF-CHEM
477 model during the MCMA-2006/MILAGRO campaign, *Atmos. Chem. Phys.*, 11(8), 3789–3809,
478 doi:10.5194/acp-11-3789-2011, 2011b.

479 Li, M., Zhang, Q., Kurokawa, J.-I., Woo, J.-H., He, K., Lu, Z., Ohara, T., Song, Y., Streets, D. G.,
480 Carmichael, G. R., Cheng, Y., Hong, C., Huo, H., Jiang, X., Kang, S., Liu, F., Su, H. and Zheng, B.:
481 MIX: a mosaic Asian anthropogenic emission inventory under the international collaboration
482 framework of the MICS-Asia and HTAP, *Atmos. Chem. Phys.*, 17(2), 935–963, doi:10.5194/acp-
483 17-935-2017, 2017b.

484 Liu, X. and Chen, B.: CLIMATIC WARMING IN THE TIBETAN PLATEAU DURING RECENT
485 DECADES, *Int. J. Climatol.*, 20, 1729–1742, 2000.

486 Liu, X., Cheng, Y., Zhang, Y., Jung, J., Sugimoto, N., Chang, S.-Y., Kim, Y. J., Fan, S. and Zeng, L.:
487 Influences of relative humidity and particle chemical composition on aerosol scattering properties
488 during the 2006 PRD campaign, *Atmos. Environ.*, 42(7), 1525–1536,
489 doi:10.1016/j.atmosenv.2007.10.077, 2008.

490 Miao, Y., Guo, J., Liu, S., Liu, H., Li, Z., Zhang, W. and Zhai, P.: Classification of summertime
491 synoptic patterns in Beijing and their associations with boundary layer structure affecting aerosol
492 pollution, *Atmos. Chem. Phys.*, 17(4), 3097–3110, doi:10.5194/acp-17-3097-2017, 2017.

493 Qiao, X., Guo, H., Tang, Y., Wang, P., Deng, W., Zhao, X., Hu, J., Ying, Q. and Zhang, H.: Local
494 and regional contributions to fine particulate matter in the 18 cities of Sichuan Basin, southwestern
495 China, *Atmos. Chem. Phys.*, 19(9), 5791–5803, doi:10.5194/acp-19-5791-2019, 2019.

496 Rangwala, I., Miller, J. R. and Xu, M.: Warming in the Tibetan Plateau: Possible influences of the
497 changes in surface water vapor, *Geophys. Res. Lett.*, 36(6), 5–6, doi:10.1029/2009GL037245, 2009.

498 Su, T., Li, Z. and Kahn, R.: Relationships between the planetary boundary layer height and surface
499 pollutants derived from lidar observations over China: regional pattern and influencing factors,
500 *Atmos. Chem. Phys.*, 18(21), 15921–15935, doi:10.5194/acp-18-15921-2018, 2018.

501 Tao, J., Zhang, L., Cao, J. and Zhang, R.: A review of current knowledge concerning PM
502 2.5 chemical composition, aerosol optical properties and their relationships across China, *Atmos.*
503 *Chem. Phys.*, 17(15), 9485–9518, doi:10.5194/acp-17-9485-2017, 2017.

504 Tie, X., Huang, R.-J., Cao, J., Zhang, Q., Cheng, Y., Su, H., Di Chang, schl, U. P. X., Hoffmann, T.,
505 Dusek, U., Li, G., Worsnop, D. R. and Dowd, C. D. O. X.: Severe Pollution in China Amplified by
506 Atmospheric Moisture, *Sci. Rep.*, 1–8, doi:10.1038/s41598-017-15909-1, 2017.

507 Tie, X., Madronich, S., Li, G., Ying, Z., Weinheimer, A., Apel, E. and Campos, T.: Simulation of
508 Mexico City plumes during the MIRAGE-Mex field campaign using the WRF-Chem model, *Atmos.*
509 *Chem. Phys.*, 9(14), 4621–4638, doi:10.5194/acp-9-4621-2009, 2009.

510 Tie, X., Madronich, S., Li, G., Ying, Z., Zhang, R., Garcia, A. R., Lee-Taylor, J. and Liu, Y.:
511 Characterizations of chemical oxidants in Mexico City: A regional chemical dynamical model
512 (WRF-Chem) study, *Atmos. Environ.*, 41(9), 1989–2008, doi:10.1016/j.atmosenv.2006.10.053,
513 2007.

514 Tie, X., Madronich, S., Walters, S., Zhang, R., Rasch, P. and Collins, W.: Effect of clouds on
515 photolysis and oxidants in the troposphere, *J. Geophys. Res.*, 108(D20), 4642,
516 doi:10.1029/2003JD003659, 2003.

517 Tie, X., Sasha, M., Stacy, W., David, E., Paul, G., Natalie, M., Renyi, Z., Lou, C. and Guy, B.:

518 Assessment of the global impact of aerosols on tropospheric oxidants, *J. Geophys. Res.*,
519 110(D03204), 13,791, doi:10.1029/2004JD005359, 2005.

520 Tie, X., Zhang, Q., He, H., Cao, J., Han, S., Gao, Y., Li, X. and Jia, X. C.: A budget analysis of the
521 formation of haze in Beijing, *Atmos. Environ.*, 100, 25–36, doi:10.1016/j.atmosenv.2014.10.038,
522 2015.

523 Tsangari, H., Paschalidou, A. K., Kassomenos, A. P., Vardoulakis, S., Heaviside, C., Georgiou, K.
524 E. and Yamasaki, E. N.: Extreme weather and air pollution effects on cardiovascular and respiratory
525 hospital admissions in Cyprus, *Science of The Total Environment*, 542(Part A), 247–253,
526 doi:10.1016/j.scitotenv.2015.10.106, 2016.

527 Wang, G., Zhang, R., Gomez, M. E., Yang, L., Levy Zamora, M., Hu, M., Lin, Y., Peng, J., Guo, S.,
528 Meng, J., Li, J., Cheng, C., Hu, T., Ren, Y., Wang, Y., Gao, J., Cao, J., An, Z., Zhou, W., Li, G.,
529 Wang, J., Tian, P., Marrero-Ortiz, W., Secrest, J., Du, Z., Zheng, J., Shang, D., Zeng, L., Shao, M.,
530 Wang, W., Huang, Y., Wang, Y., Zhu, Y., Li, Y., Hu, J., Pan, B., Cai, L., Cheng, Y., Ji, Y., Zhang, F.,
531 Rosenfeld, D., Liss, P. S., Duce, R. A., Kolb, C. E. and Molina, M. J.: Persistent sulfate formation
532 from London Fog to Chinese haze, *P. Natl. Acad. Sci. USA*, 113(48), 13630–13635,
533 doi:10.1073/pnas.1616540113, 2016.

534 Wang, H., Tian, M., Chen, Y., Shi, G., Liu, Y., Yang, F., Zhang, L., Deng, L., Yu, J., Peng, C. and
535 Cao, X.: Seasonal characteristics, formation mechanisms and source origins of PM_{2.5} in two
536 megacities in Sichuan Basin, China, *Atmos. Chem. Phys.*, 18(2), 865–881, doi:10.5194/acp-18-865-
537 2018, 2018.

538 Wesely, M. L.: Parameterization of surface resistances to gaseous dry deposition in regional-scale
539 numerical models, *Atmospheric Environment* (1967), 23(6), 1293–1304, doi:10.1016/0004-
540 6981(89)90153-4, 1989.

541 Xu, J., Chang, L., Yan, F. and He, J.: Role of climate anomalies on decadal variation in the
542 occurrence of wintertime haze in the Yangtze River Delta, China, *Science of The Total Environment*,
543 599-600, 918–925, doi:10.1016/j.scitotenv.2017.05.015, 2017.

544 Xu, X., Zhao, T., Liu, F., Gong, S. L., Kristovich, D., Lu, C., Guo, Y., Cheng, X., Wang, Y. and Ding,
545 G.: Climate modulation of the Tibetan Plateau on haze in China, *Atmos. Chem. Phys.*, 16(3), 1365–
546 1375, doi:10.5194/acp-16-1365-2016, 2016.

547 Yang, F., Tan, J., Zhao, Q., Du, Z., He, K., Ma, Y., Duan, F., Chen, G. and Zhao, Q.: Characteristics
548 of PM 2.5 speciation in representative megacities and across China, *Atmos. Chem. Phys.*, 11(11),
549 5207–5219, doi:10.5194/acp-11-5207-2011, 2011.

550 Zhang, H., Wang, Y., Park, T.-W. and Deng, Y.: Quantifying the relationship between extreme air
551 pollution events and extreme weather events, *Atmospheric Research*, 1–48,
552 doi:10.1016/j.atmosres.2016.11.010, 2016.

553 Zhang, Q., Streets, D. G., Carmichael, G. R., He, K. B., Huo, H., Kannari, A., Klimont, Z., Park, I.
554 S., Reddy, S., Fu, J. S., Chen, D., Duan, L., Lei, Y., Wang, L. T. and Yao, Z. L.: Asian emissions in
555 2006 for the NASA INTEX-B mission, *Atmos. Chem. Phys.*, 9(14), 5131–5153, doi:10.5194/acp-
556 9-5131-2009, 2009.

557 Zhao, P., Li, Y., Guo, X., Xu, X., Liu, Y., Tang, S., Xiao, W., Shi, C., Ma, Y., Yu, X., Liu, H., Jia, L.,
558 Chen, Y., Liu, Y., Li, J., Luo, D., Cao, Y., Zheng, X., Chen, J., Xiao, A., Yuan, F., Chen, D., Pang,
559 Y., Hu, Z., Zhang, S., Dong, L., Hu, J., Han, S. and Zhou, X.: The Tibetan Plateau Surface-
560 Atmosphere Coupling System and Its Weather and Climate Effects: The Third Tibetan Plateau
561 Atmospheric Science Experiment, *J Meteorol Res.*, 33(3), 375–399, doi:10.1007/s13351-019-8602-
562 3, 2019.

563 Zhao, S., Feng, T., Tie, X., Long, X., Li, G., Cao, J., Zhou, W. and An, Z.: Impact of Climate Change
564 on Siberian High and Wintertime Air Pollution in China in Past Two Decades, *Earth's Future*, 6,
565 118–133, doi:10.1002/2017EF000682, 2018.

566 Zhao, S., Tie, X., Cao, J. and Zhang, Q.: Impacts of mountains on black carbon aerosol under
567 different synoptic meteorology conditions in the Guanzhong region, China, *Atmospheric Research*,
568 164-165(C), 286–296, doi:10.1016/j.atmosres.2015.05.016, 2015.

569 Zhu, Q., Shou, S. and Tang, D.: *Principles and methods of weather*, 4 ed., Beijing. 2000.

570 Zou, Y., Wang, Y., Zhang, Y. and Koo, J.-H.: Arctic sea ice, Eurasia snow, and extreme winter haze
571 in China, *Sci. Adv.*, 3(3), e1602751–9, doi:10.1126/sciadv.1602751, 2017.

572

Figure captions

Figure 1 (a) Location map of the Tibetan Plateau (the region surrounded by the dark line) and the Sichuan Basin (the region surrounded by the gray line). (b) The model domain and the distribution of weather stations marked in the triangles over the Tibetan Plateau and air quality stations marked in the circles over the Sichuan Basin.

Figure 2 Trends of observational winter (Dec-Jan-Feb) mean temperature anomaly recorded by 10 weather stations over the Tibetan Plateau during the last four decades (1979-2017).

Figure 3 Trends of ERA-interim reanalysis winter mean temperature over the Tibetan Plateau from 1979 to 2017. The dotted regions show statistical significance with 95% confidence level (p -value < 0.05) from the Student's t test.

Figure 4 Comparison between the observed (black dots) and simulated (blue line) hourly O_3 ($\mu\text{g m}^{-3}$), CO (mg m^{-3}) and $PM_{2.5}$ mass concentration ($\mu\text{g m}^{-3}$) over the Sichuan Basin in January 2014.

Figure 5 Time series of **PM_{2.5} concentration** over the Sichuan Basin, the baseline simulation is selected in January 2014 and the sensitivity simulation in which 2°C warming occurs over the Tibetan Plateau relative to the baseline simulation.

Figure 6 Comparison of chemical composition of $PM_{2.5}$ concentration between the baseline simulation (red bar) and sensitivity simulation (blue bar) over the Sichuan Basin.

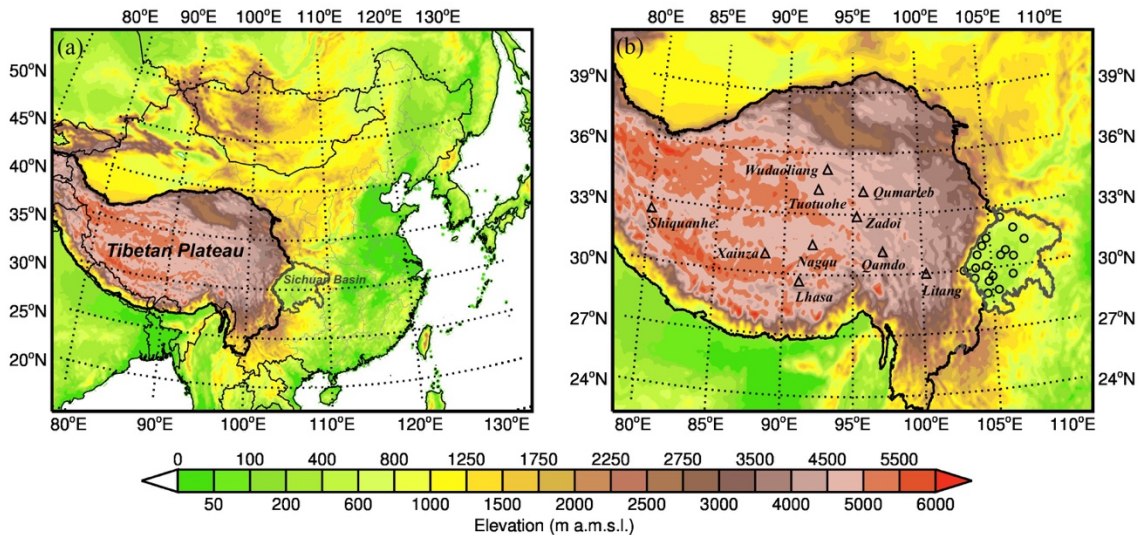
Figure 7 Difference in spatial distributions of surface PM_{2.5} concentration (shading) and winds (arrows) between the sensitivity simulation and baseline simulation. The negative shows PM_{2.5} concentration decreases and the positive shows PM_{2.5} concentration increases when the Tibetan Plateau is 2°C warming.

Figure 8 Comparison of spatial distributions of sea level pressure (SLP) between the (a) baseline simulation and (b) sensitivity simulation over the Tibetan Plateau and Sichuan Basin. (c) The SLPs over the plateau and basin decrease while the plateau becomes 2°C warming.

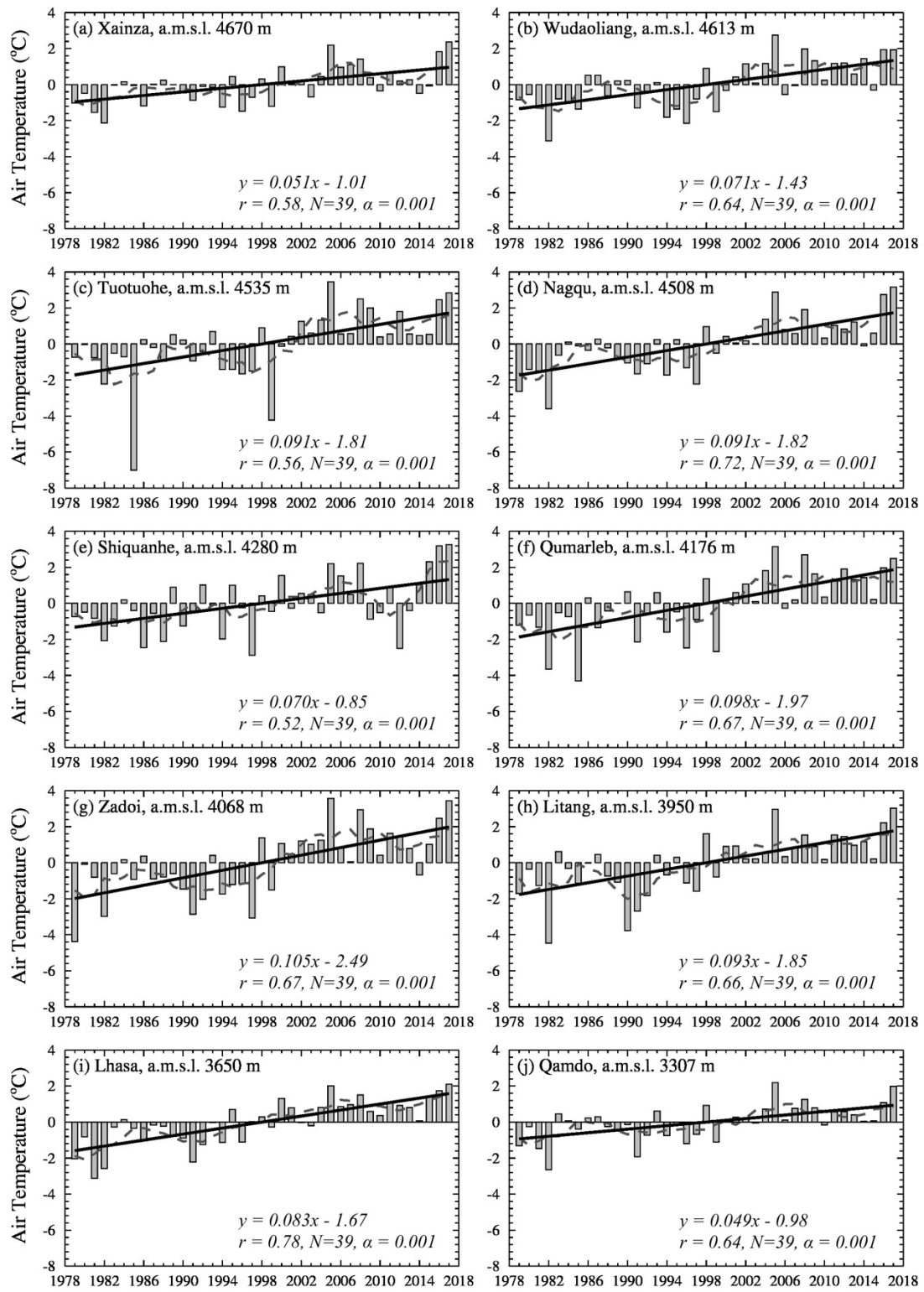
Figure 9 Spatial change in the PBL height induced by 2°C warming over the Tibetan Plateau. The positive shows the PBL height increases while the negative shows the PBL height decreases.

Figure 10 Vertical profiles of changes in temperature (shading and gray contour) and winds (arrows) along 30°N in January 2014. The gray shaded area presents topography. The green box for the Sichuan Basin, and the red solid (baseline simulation) and dash (sensitivity simulation) lines for the PBL height. (a) The Tibetan Plateau and Sichuan Basin, and (b) The Sichuan Basin.

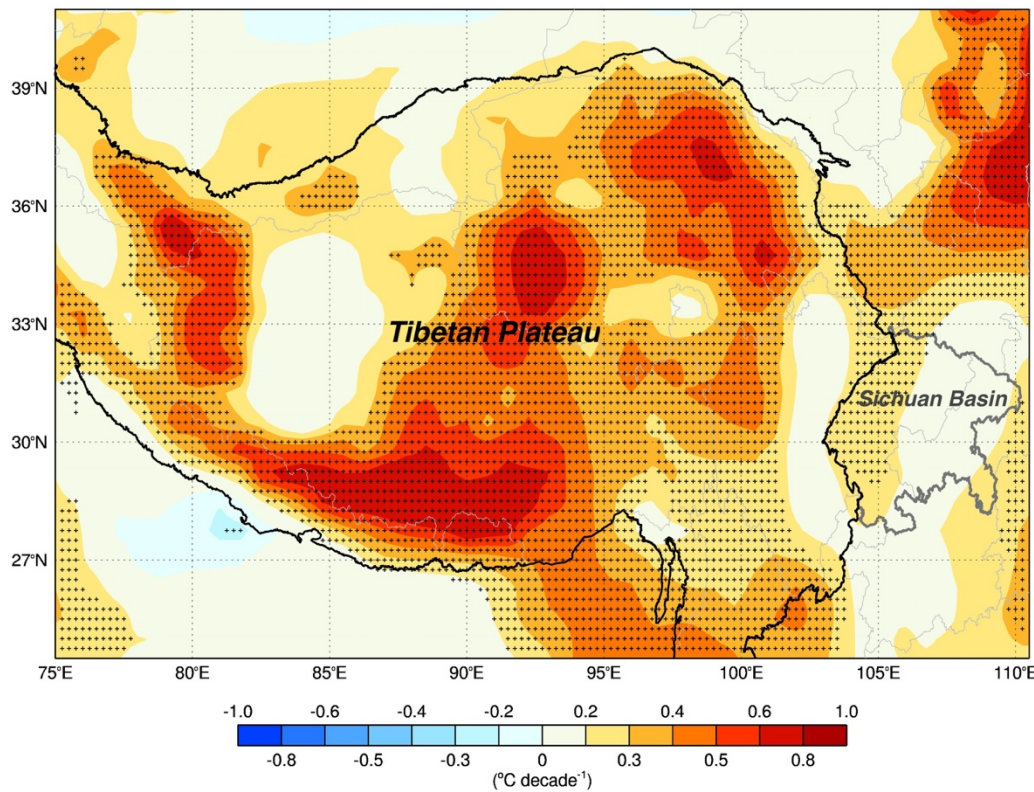
Figure 11 Comparison of spatial distributions of relative humidity (RH) between the (a) baseline simulation and (b) sensitivity simulation over the Tibetan Plateau and Sichuan Basin. (c) Spatial changes in RH after the plateau becomes 2°C warming, and the positive shows the RH increases while the negative shows the RH decreases.



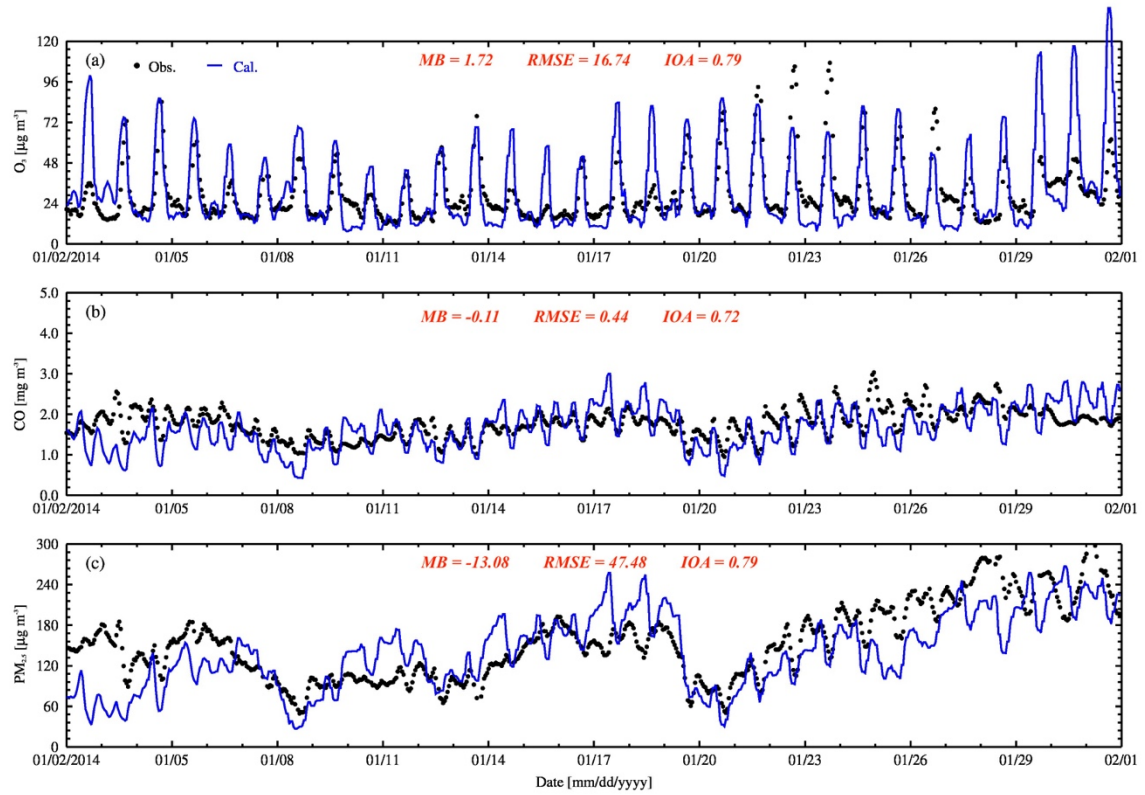
611 **Figure 1** (a) Location map of the Tibetan Plateau (the region surrounded by the dark line) and the Sichuan
 612 Basin (the region surrounded by the gray line). (b) The model domain and the distribution of weather stations
 613 marked in the triangles over the Tibetan Plateau and air quality stations marked in the circles over the Sichuan
 614 Basin.



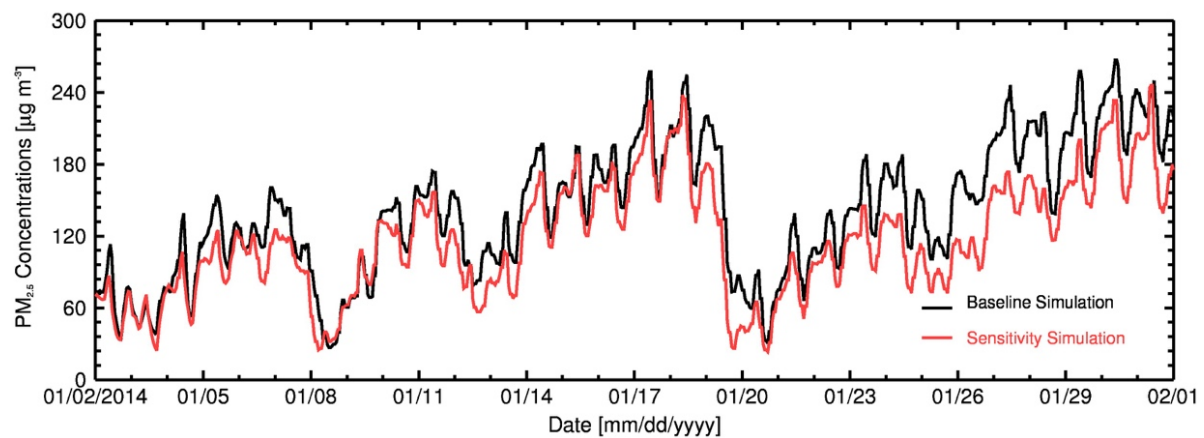
617 **Figure 2** Trends of observational winter (Dec-Jan-Feb) mean temperature anomaly recorded by 10 weather
 618 stations over the Tibetan Plateau during the last four decades (1979-2017).



621 **Figure 3** Trends of ERA-interim reanalysis winter mean temperature over the Tibetan Plateau from 1979 to
 622 2017. The dotted regions show statistical significance with 95% confidence level (p -value < 0.05) from the
 623 Student's t test.

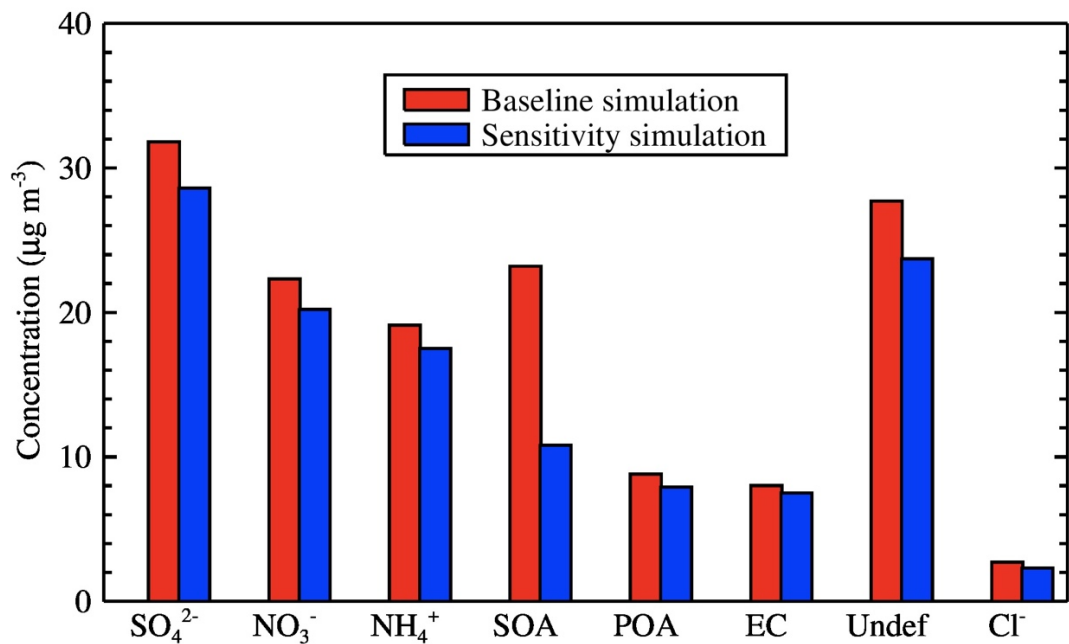


626 **Figure 4** Comparison between the observed (black dots) and simulated (blue line) hourly O₃ ($\mu\text{g m}^{-3}$), CO
 627 (mg m^{-3}) and PM_{2.5} mass concentration ($\mu\text{g m}^{-3}$) over the Sichuan Basin in January 2014.



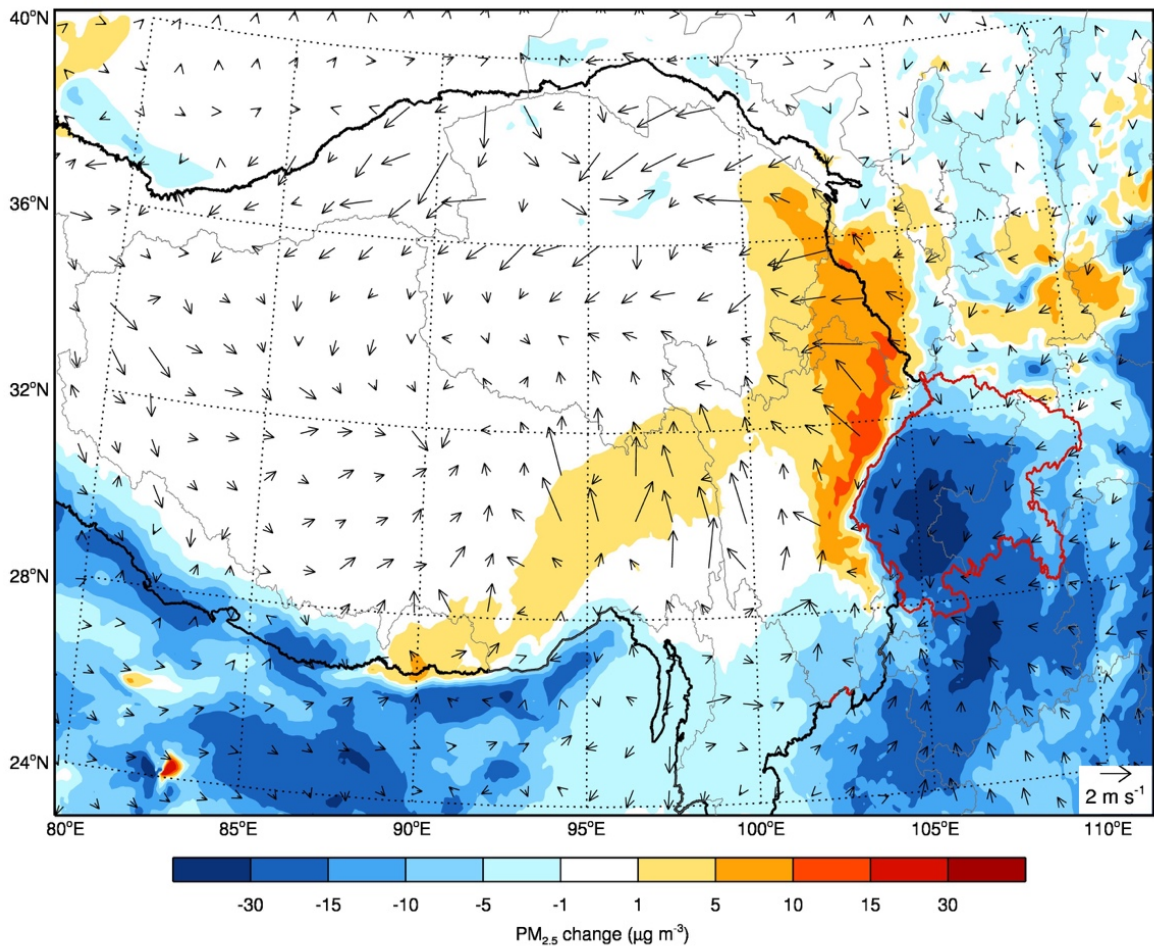
631 **Figure 5** Time series of $\text{PM}_{2.5}$ concentration over the Sichuan Basin, the baseline simulation is selected in
632 January 2014 and the sensitivity simulation in which 2°C warming occurs over the Tibetan Plateau relative
633 to the baseline simulation.

634

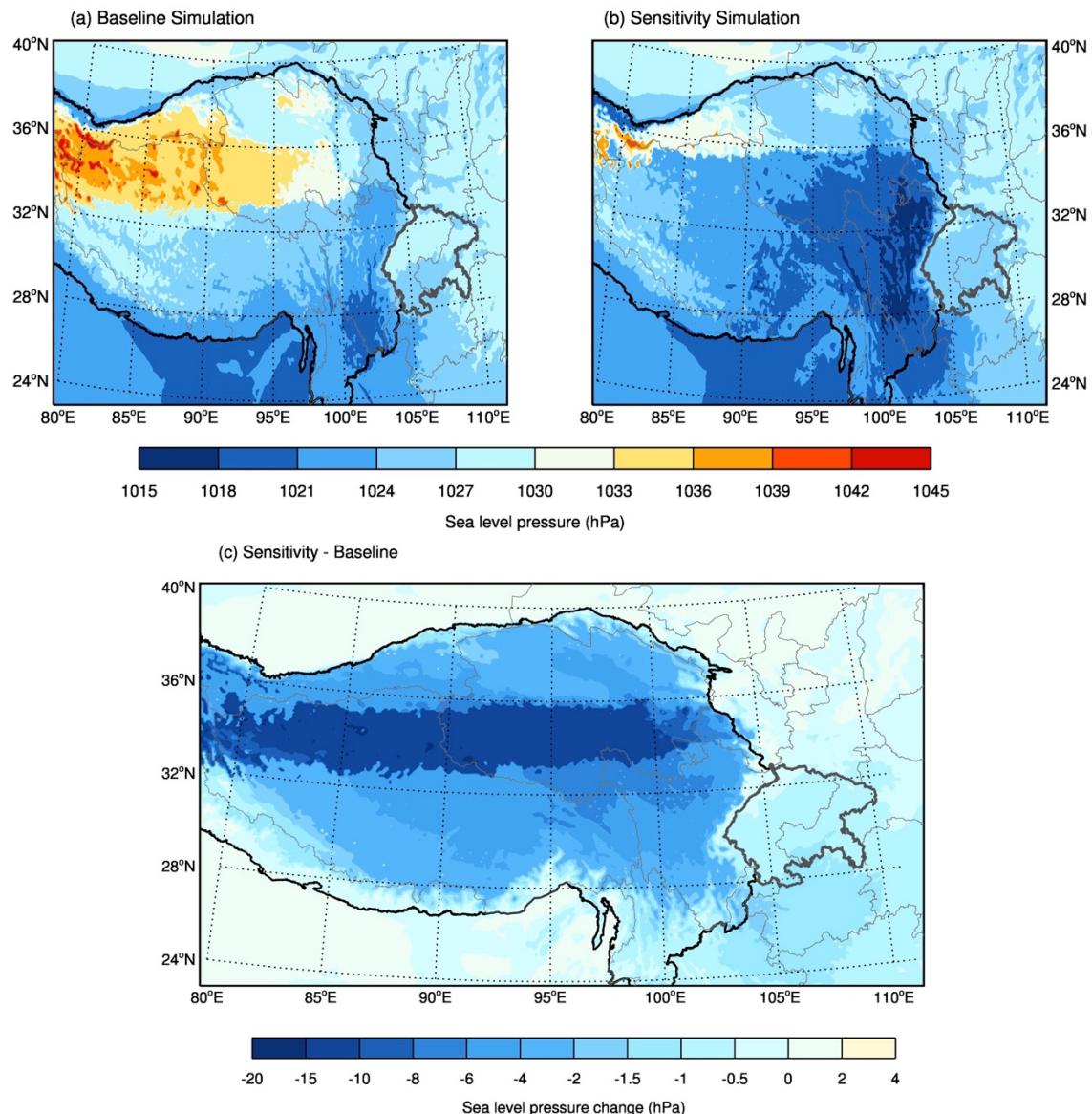


635

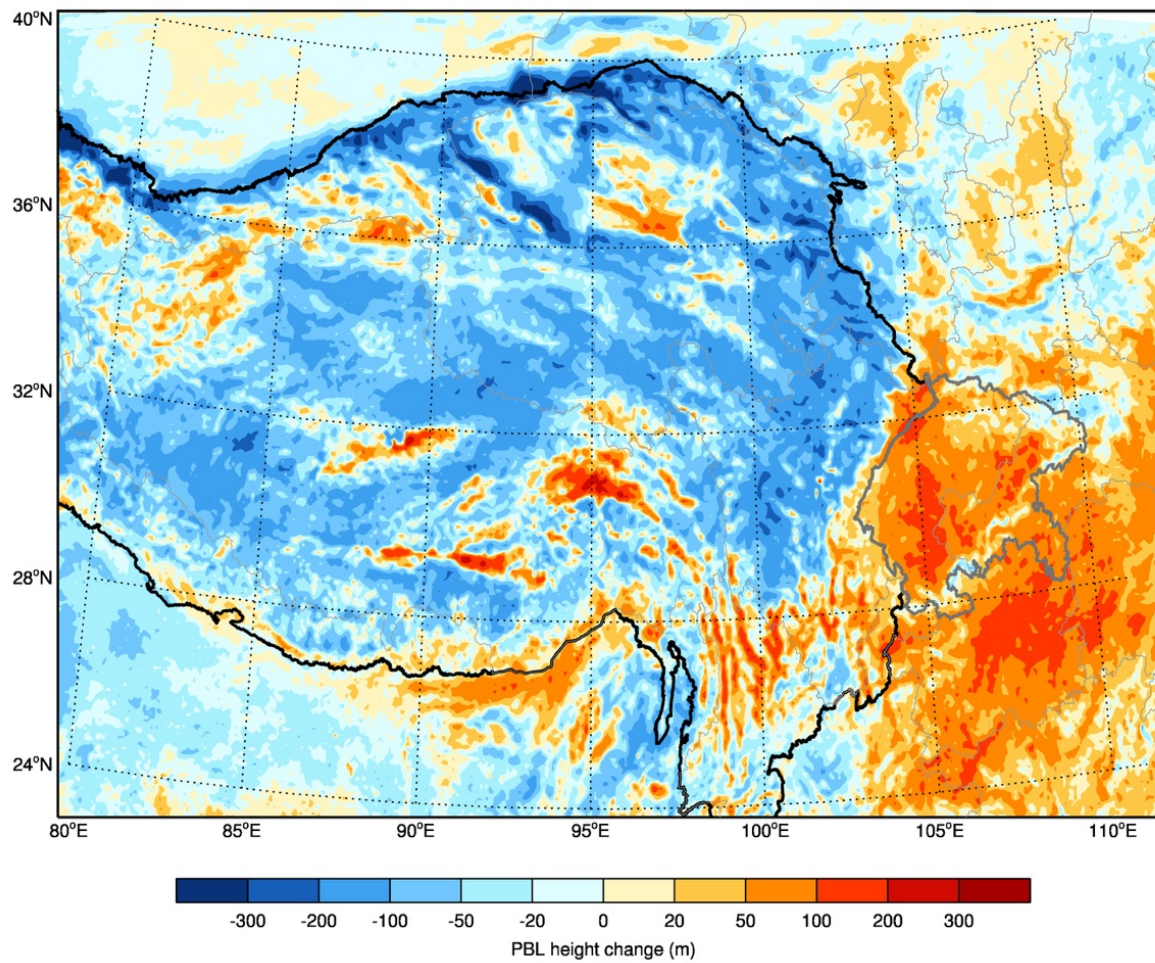
636 **Figure 6** Comparison of chemical composition of PM_{2.5} concentration between the baseline simulation (red
637 bar) and sensitivity simulation (blue bar) over the Sichuan Basin.



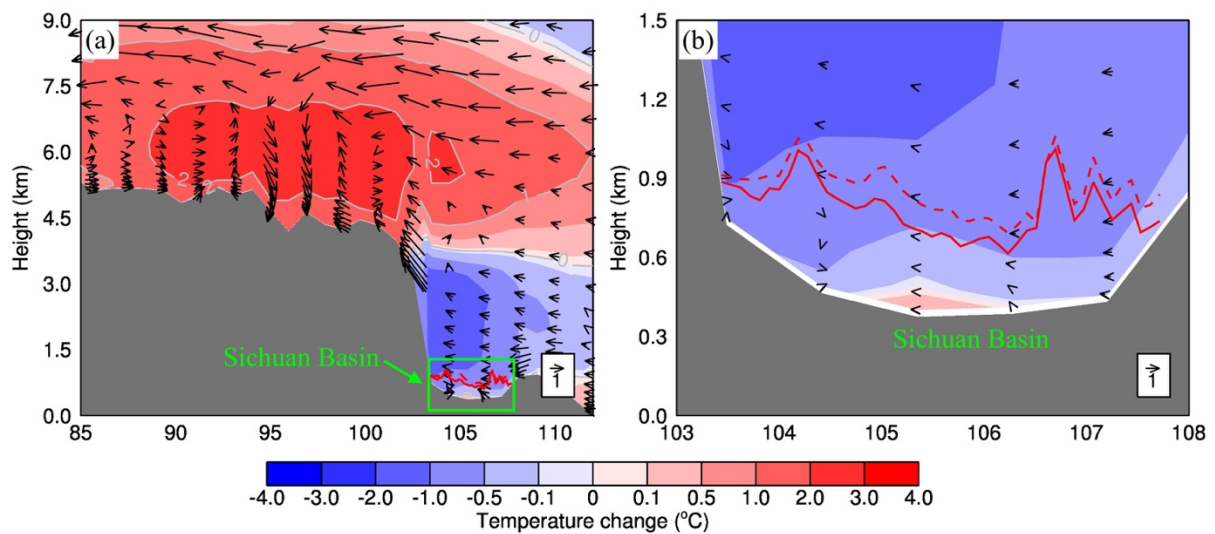
640 **Figure 7** Difference in spatial distributions of surface PM_{2.5} concentration (shading)
 641 and winds (arrows) between the sensitivity simulation and baseline simulation. The negative shows PM_{2.5} concentration
 642 decreases and the positive shows PM_{2.5} concentrations increases when the Tibetan Plateau is 2°C warming.



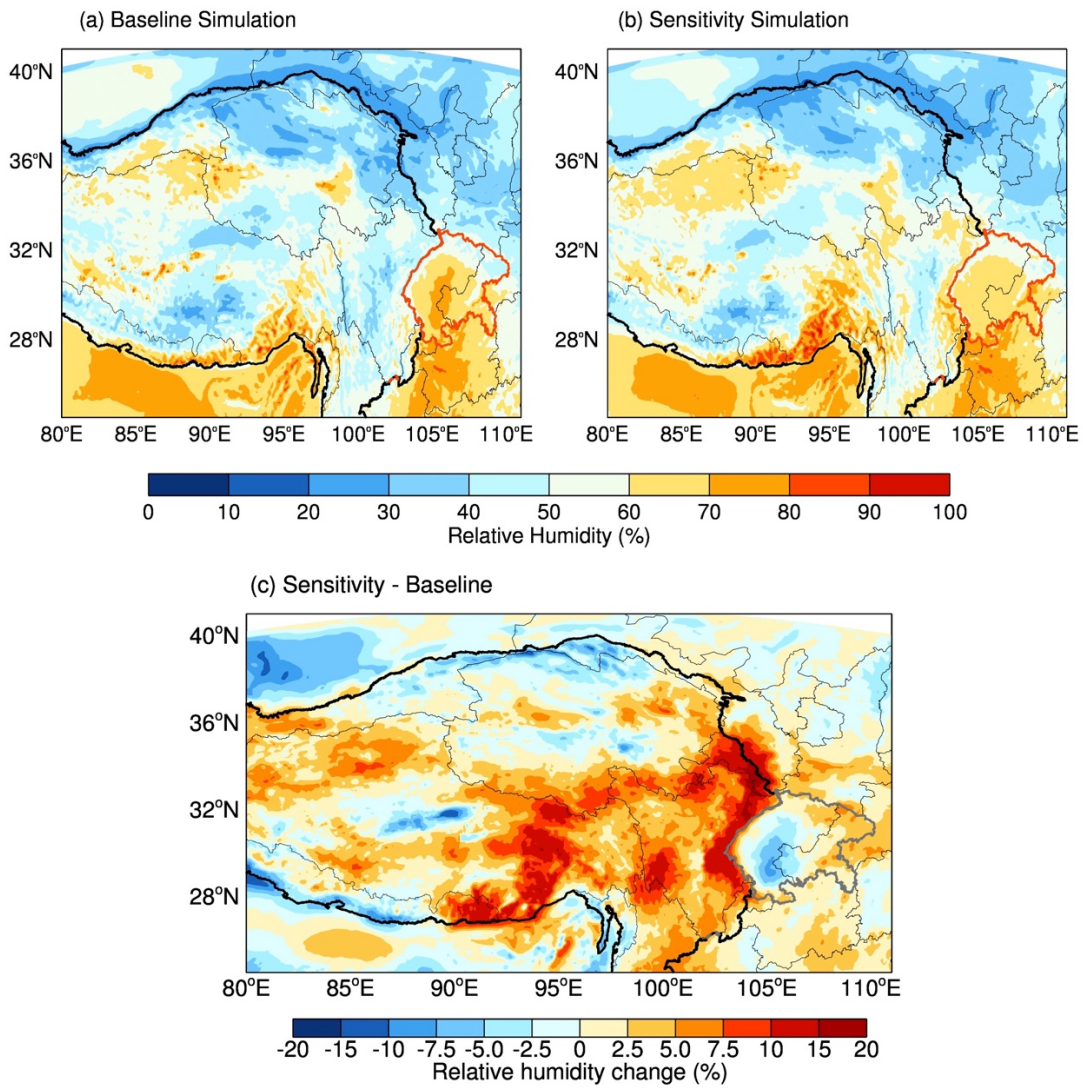
645 **Figure 8** Comparison of spatial distributions of sea level pressure (SLP) between the (a) baseline simulation
 646 and (b) sensitivity simulation over the Tibetan Plateau and Sichuan Basin. (c) The SLPs over the plateau and
 647 basin decrease while the plateau becomes 2°C warming.



650 **Figure 9** Spatial change in the PBL height induced by 2°C warming over the **Tibetan Plateau**. The positive
 651 shows the PBL height increases while the negative shows the PBL height decreases.



654 **Figure 10** Vertical profiles of changes in temperature (color shading and gray contour) and winds (arrows)
 655 along 30°N in January 2014. The gray shaded area presents topography. The green box for the Sichuan Basin,
 656 and the red solid (baseline simulation) and dash (sensitivity simulation) lines for the PBL height. (a) The
 657 Tibetan Plateau and Sichuan Basin, and (b) The Sichuan Basin.



660 **Figure 11** Comparison of spatial distributions of relative humidity (RH) between the (a) baseline
 661 simulation and (b) sensitivity simulation over the Tibetan Plateau and Sichuan Basin. (c) Spatial
 662 changes in RH after the plateau becomes 2°C warming, and the positive shows the RH increases
 663 while the negative shows the RH decreases.